

~~SECRET~~

14-00000

POST FLIGHT EVALUATION
OF RECOVERED SRV HARDWARE

PROGRAM [REDACTED]

JANUARY, 1965

Prepared By
Re-Entry Systems and Technology Section

Approved By

[REDACTED] Manager

Space Systems Programs

GENERAL (GE) ELECTRIC
Re-Entry Systems Department
A Department of the Missile and Space Division
3198 Chestnut Street
Philadelphia 4, Penna.

65-10-150

~~SECRET~~

FOREWARD

This evaluation was performed in support of Program [REDACTED] by the Re-Entry Systems and Technology Section, Re-entry Systems Department, General Electric Company, Philadelphia, Pennsylvania. Technical direction was provided by [REDACTED] System Engineer, Program [REDACTED]. Other principal contributors were: [REDACTED]

The cooperation and assistance of the Space Systems Division, United States Air Force is acknowledged.

ABSTRACT

Recovered hardware (debris) from a Program [REDACTED] re-entry vehicle were furnished to the Re-Entry Systems Department for evaluation. This vehicle had flown ^{thirty} ~~seventy~~ days in orbit before commencing a re-entry trajectory because of atmospheric drag effects. Exposure to the tropical ~~atmosphere~~ ^{environment} followed impact. Debris consisted of sections of the forebody and attached hardware, and pieces of the thermal cover and parachute.

The phenolic-nylon heat shield had evidence of: (1) local cracking in orbit, (2) development of a protrusion during orbit or early re-entry, and (3) curling at edges adjacent to stress relief grooves during re-entry. Miss performance capability is not limited by these conditions. Shield degradation during re-entry matched semi-empirical correlations developed from previous data within reasonable tolerances. Degradation rate parameters were determined from shield material exposed to the actual re-entry environment. Performance of the current gap filler was confirmed. Parts, parachute, and thermal cover evaluations suggest that the afterbody was not directly exposed to re-entry heating while tumbling, or prior to R/V stabilization and separation. Magnet mounting ring and ring-to-liner bond investigations indicated satisfactory performance.

Results confirm adequacy of the present design and vehicle quality.

TABLE OF CONTENTS

Page

FOREWORD

ABSTRACT

TABLE OF CONTENTS

I. INTRODUCTION

II. FLIGHT PROFILE AND CONFIGURATION

III. RECOVERED DEBRIS

IV. DEBRIS EVALUATION

A. Orbit and Upper-Atmospheric Flight

B. Re-Entry and Impact

1. Thermodynamic Performance

2. Materials Performance

a. Degradation Kinetics

b. Parts Evaluation

V. CONCLUSIONS

VI. REFERENCES

LIST OF FIGURES

Page

- Figure 0 - Orbit Injection Configuration
- Figure 1 - Photograph of Forebody Assembly Section Showing
Eroded Crater-Like Formation
- Figure 2 - Photograph of Forebody Assembly Cross-Section
Showing Shield Edge Cooling and Capsule Guides
- Figure 3 - Photograph of Forebody Assembly Sectional Showing
Ablated Heat Shield Surface
- Figure 4 - Minimum Temperature Location on Shield During Earth-
Oriented Orbital Flight
- Figure 5 - Re-Entry Path Angle, Velocity, and Time vs. Altitude
- Figure 6 - Re-Entry Mach Number, Dynamic Pressure, and Axial Load
vs. Altitude
- Figure 7 - Measured Shield Degradation vs. Axial Station
- Figure 8 - Shield Degradation vs. Integrated Heat Flux
- Figure 9 - Integrated Heat Flux vs. Re-Entry Heating Parameter
- Figure 10 - Sketch of Shield Cross-Section Showing Edge Curling

- Figure 11 - DTA Thermogram of Top Third Phenolic-Nylon Sample
- Figure 12 - DTA Thermogram of Middle Third Phenolic-Nylon Sample
- Figure 13 - DTA Thermogram of Bottom Third Phenolic-Nylon Sample
- Figure 14 - TGA Thermogram of Reference Phenolic-Nylon Sample
- Figure 15 - TGA Thermogram of Top Third Phenolic-Nylon Sample
- Figure 16 - TGA Thermogram of Middle Third Phenolic-Nylon Sample
- Figure 17 - TGA Thermogram of Bottom Third Phenolic-Nylon Sample
- Figure 18 - TGA Residual Weight Fraction Ratio at Selected Temperature
Points vs. Sampling Depth
- Figure 19 - DTA Temperature Difference Indicated at Selected Temperature
Points vs. Sampling Depth
- Figure 20 - SRV Location of Parts Sectioned and Evaluated

~~SECRET~~

~~SECRET~~
LIST OF TABLES

(6)

Page

Table I - Shield Degradation Measurements

Table II - Arrhenius Parameters

~~SECRET~~

I. INTRODUCTION

Recovered re-entry vehicles and materials can provide information and data which cannot now be duplicated by ground tests. Ground simulations of flight environments are only limited simple approximations because of facility and technology capabilities, knowledge of flight environmental parameters, ambient natural conditions, and economy of resources. Capability for direct or remote observation during flight is also limited. Therefore the present evaluation was performed with the following objectives:

1. identification of areas where product improvements might be made
2. observation and measurement of response and performance in actual flight environments
3. increased understanding of operational capabilities
4. advancement of technology resulting from application of new data and upgrading of design techniques.

II FLIGHT PROFILE AND CONFIGURATION

The hardware received was from the RV (apparently "A" RV) of a [REDACTED] configuration spacecraft launched from the Air Force Western Test Range on a Thrust Augmented Thor Booster. Launch data, and orbital elements and data on injection were:

- a. date of launch - April 27, 1964
- b. time of launch - 2325 Z (1525 PST)
- c. height of apogee - 251.8 miles
- d. height of perigee - 99.2 miles
- e. inclination - 79.92° (prograde)
- f. period - 90.87 minutes
- g. eccentricity - .0211

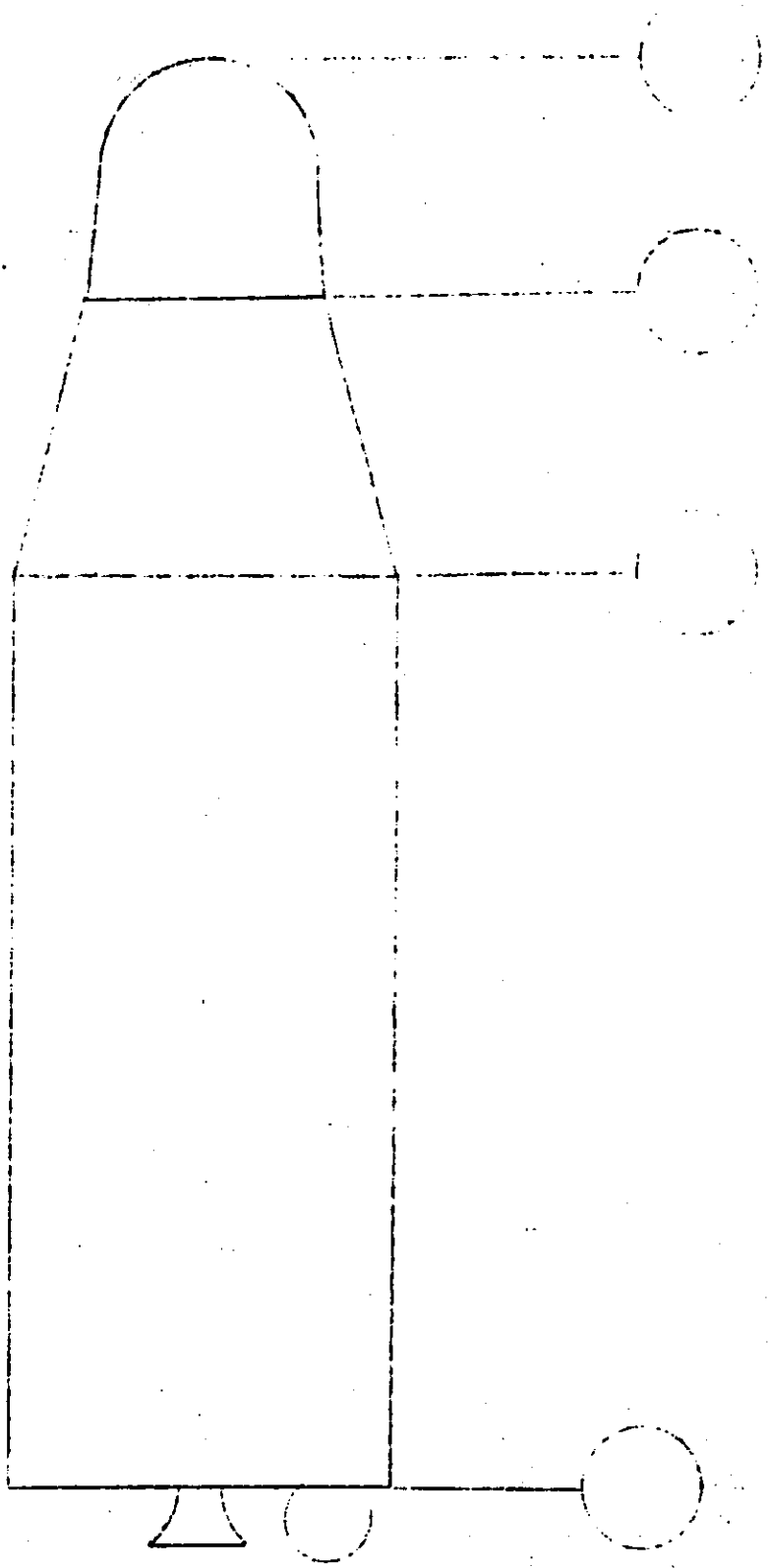
The spacecraft was re-oriented and stabilized after injection, and maintained stabilization and earth-orientation until the seventy-second (72nd) orbit, at which time the tumbling

00-7

mode was commenced. (The "A" RV could not be separated according to plan at the end of this first orbital mission phase.) The spacecraft was re-stabilized on the two hundred and forty-sixth (246th) orbit, but lost stabilization within two days afterwards because of propellant gas depletion. Thirty days after injection, the spacecraft orbit injection configuration (see Figure 0) commenced a re-entry trajectory because of atmospheric drag effects. Impact was in Venezuela, S.A. on May 26, 1964. ~~Trace of the~~ a South to North trace, ~~the~~ and impact point coordinates were 8° north latitude, 67° west. Radar provided continuous tracking. At some point on the spacecraft descended in its trajectory, the radar indicated a change from smooth to

~~SECRET~~

FIGURE C



~~SECRET~~

CHEVROLET INJECTION CONFIGURATION

~~SECRET~~

Handwritten notes:
31
30
32
33
34
35
36
37
38
39
40
41
42
43
44
45
46
47
48
49
50
51
52
53
54
55
56
57
58
59
60
61
62
63
64
65
66
67
68
69
70
71
72
73
74
75
76
77
78
79
80
81
82
83
84
85
86
87
88
89
90
91
92
93
94
95
96
97
98
99
100

~~SECRET~~
~~SECRET~~

multiple object return. Specific location and altitude at this point, and duration of tropical exposure after impact are unknown.

~~SECRET~~
~~SECRET~~

III. RECOVERED DEBRIS

In composite, the pieces received constituted sections of a forebody assembly (GE drawing #198R301) with certain higher assembly items installed, and several portions of the parachute and thermal cover. Included were:

- a. heat shield assembly: phenolic-nylon ablative shell and phenolic-glass structural liner, silicone rubber gap filler (GE drawing #226E590)
- b. aft shield ring: phenolic-glass (GE drawing #679D122)
- c. mounting ring: magnesium alloy ^{ZE41A} ZE41A (GE drawing #198R306)
- d. microswitch: component with aluminum bracket (GE drawing #692D911)
- e. interface lug: steel part coated with solid film lubricant, molybdenum disulfide in an alkyd binder (GE drawing #102B7805)
- f. WJ1 interface harness connector: [REDACTED] part PC07H-22-55P
- g. parachute: portions of fabric (GFE)
- h. thermal cover: phenolic-glass (Pyropreg) (GE drawing #226E590)
- i. capsule guides; phenolic-glass with steel facings (GE Drawings #887C525 and #692D925)

Photographs of portions of the recovered forebody sections, Figures 1, 2, and 3, show the general condition of the heat shield and other materials received. Other portions of the shield were deeply impressed with soil. With the exception of a badly damaged and soiled section which included regions of the nose cap periphery, returned shield sections were from conical frustum of the heat shield assembly.

IV. DEBRIS EVALUATION

A. Orbit and Upper-Atmospheric Flight

Visual examination of the phenolic-nylon heat shield revealed the typical "dried mud flat" appearance of an ablative material after re-entry and cool-down. Most of the random cracks (see Figure 3) were produced after re-entry when the phenolic nylon cooled down. During re-entry when the phenolic nylon is above 500°F it deforms plastically in compression so that a sudden cooling after re-entry would produce tensile cracks. This is substantiated by the fact that most of the cracks near the free edge of the phenolic nylon are meridional in direction because of high hoop compression during re-entry with very low axial compressive stresses. Most of the cracks in the hoop direction are away from the free edges where the axial compression stresses are equal or higher than the hoop compression stresses. Several cracks were observed, however, which evidently occurred during orbital flight.

Based on the launch parameters and flight profile, β angles (angle between solar vector and orbital plane) of -50° to -35° were experienced during orbit. These conditions could result in local heat shield temperatures as low as -190°F . Minimum temperature location is shown in Figure 4. By analysis (reference 1), local shield cracking would be predicted even with no degradation of material properties (shrinkage, reduction of elongation) or compressive creep due to previous elevated temperature exposure in orbit. The cracks would occur close to the stress relief grooves, in a meridional direction, with the most severe cracks developing at the aft-most stress relief groove. Considering the circumferential temperature distribution and the minimum temperature location for earth-oriented orbital flight, the predicted cracks would be confined to the small segment of the circumference experiencing near minimum temperatures (approximately 20 degrees of arc). Very few cracks would be expected, since those occurring would relieve the local stress levels.

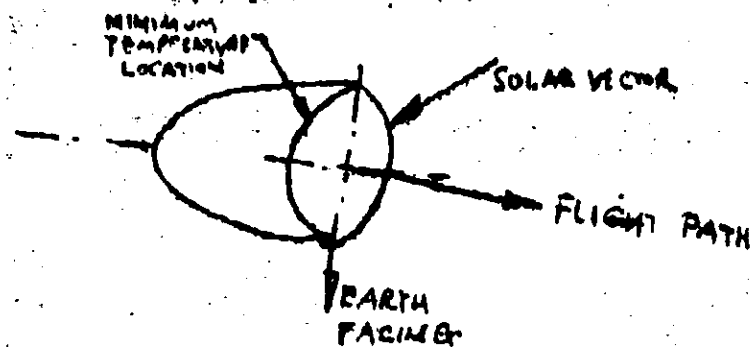


FIGURE 4

Minimum Temperature Location on Shield
During Earth-Oriented Orbital Flight

The minimum temperature region for earth-oriented flight was located on the debris and the cracks examined for charring along the edges down to the phenolic glass. Only one such crack was found in this region and upon examination of the rest of the shield circumference, only two or three other similar cracks could be found, randomly spaced around the circumference. Most of the cracks still had virgin material at the base next to the phenolic glass, indicating that these cracks occurred during the latter portion or subsequent to the re-entry heating period.

Based on the analytical predictions and on the fact that several cracks had charring along the edges down to the phenolic glass, the conclusion is reached that these cracks occurred in orbit. The random locations probably occurred due to the fact that the vehicle was stabilized in orbit for only the first four and latter two days. For most of the remaining days in orbit, the vehicle was probably tumbling. If, during this latter time, the vehicle was ^{subjected to oscillation or maneuvering} stabilized for three to five orbits, other portions of the circumference could also have been subjected to ^{very low} ~~this cold~~ temperature, thus producing the additional cracks. In any event, these meridional cracks, local to the stress relief grooves, produced by in-orbit cold temperatures, are not considered detrimental to the mission performance capability of the shield system.

A trajectory was calculated from known initial orbital conditions to impact. The orbital elements which were used are defined in Section II of this report. A constraint on the trajectory was impacting in thirty days, with the given history of stabilized and unstabilized flight. Using a Harris-Priester atmosphere, this condition was satisfied. For stabilized flight throughout the observed duration of orbit, only a small amount of decay would have resulted.

The motion behavior of the vehicle can only be a subject of speculation since the aerodynamic and mass characteristics are not known. However, it is most probable that the vehicle stabilized and the R/V separated from the rest of the orbital system at a high altitude. The R/V then continued into impact. Assuming a W/C_pA of 55 psf the trajectory parameters are given in Figures 5 and 6. This trajectory gives rise to the thermal shield weight loss which was observed.

B. Re-Entry and Impact

1. Thermodynamic Performance

a. Shield Performance

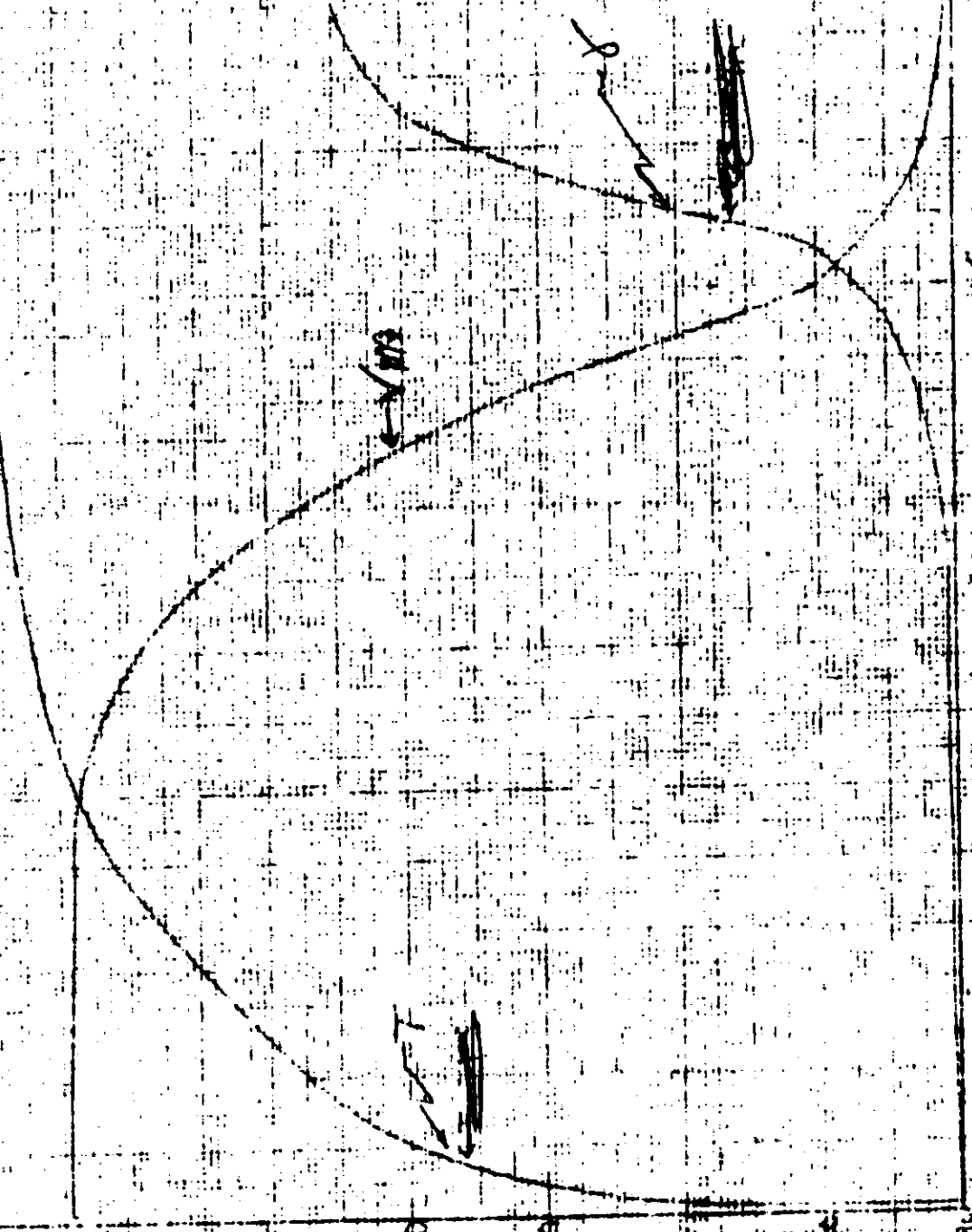
Post recovery measurements were taken from the aft frustum pieces of the vehicle heat shield to determine the extent of shield degradation. By use of previous flight data and simplified techniques, this data was translated into an estimate of the aerodynamic heating experienced by the R/V during re-entry.

Table I presents measurements taken from the recovered aft frustum pieces. By subtracting the remaining phenolic nylon thickness from the nominal design thickness of the shield, it was possible to obtain an estimate of the depth of local shield degradation. This data and similar data from R/V 38 is plotted as a function of vehicle axial length in Figure 7. It can be seen that the average debris degradation depth is greater than that of R/V 38 by 36% and 73% at Stations 23 and 18 respectively. A fair amount of debris data scatter is shown, but it is not in excess of the ³⁷~~30~~ variance indicated by extensive post recovery measurements obtained from R/V 38.

Figure 8 presents a correlation of R/V 39 degradation depth as a function of the time integrated re-entry heating. The mean degradation values of Station 18 and 23 (Figure 7) were used as an argument to enter Figure 8 so that estimates of the local heating rates could be obtained. For Station 18 the integrated heating is 3770 BTU/Ft² and at Station 23, 2350 BTU/Ft². The ratio of these two values is 63% normally, a ratio of 89% would be

FIGURE 511

REENTRY PATH, ALTITUDE, VELOCITY, AND TIME VS. ALTITUDE



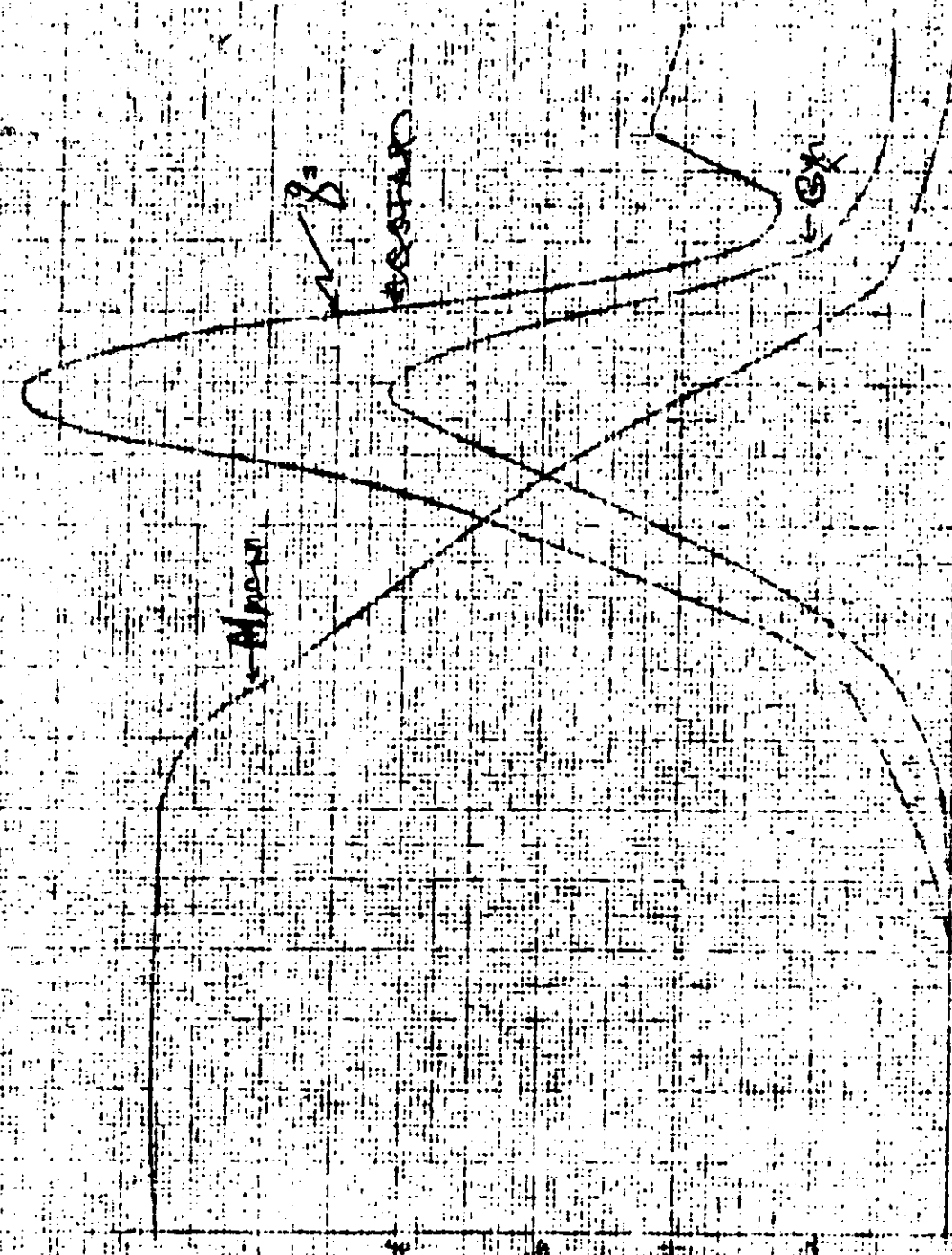
ALTITUDE (FT)

TIME (SEC)

VELOCITY (FT/SEC)

REENTRY PATH

FIGURE 6
 PRE-ENTRY MACH NUMBER, DYNAMIC PRESSURE, AND AXIAL LOAD VS. ALTITUDE



Altitude (ft) $\times 10^3$

TABLE I
SHIELD DEGRADATION MEASUREMENTS

L O C A T I O N			M A T E R I A L	THICKNESS	IN.
SAMPLE NO	STATION* IN.	CLOCK ANGLE DEG.	CHAR + VIRGIN PHENOLIC NYLON	VIRGIN PHENOLIC NYLON REMAINING	DEPTH OF DEGRADATION **
1	17.91	315°	0.138	0.097	0.12
1	17.91	315	0.162	0.136	0.08
2	23.4	45	0.187	0.147	0.07
3	18.4	130	0.212	0.161	0.06
4	18.4	150	0.145	0.121	0.10
5	23.4	315	0.194	0.136	0.08
6	23.4	20	0.220	0.176	0.04
6	23.4	20	0.262	0.174	0.05
7	23.4	135	0.206	0.160	0.06
8	23.4	160	0.178	0.153	0.07

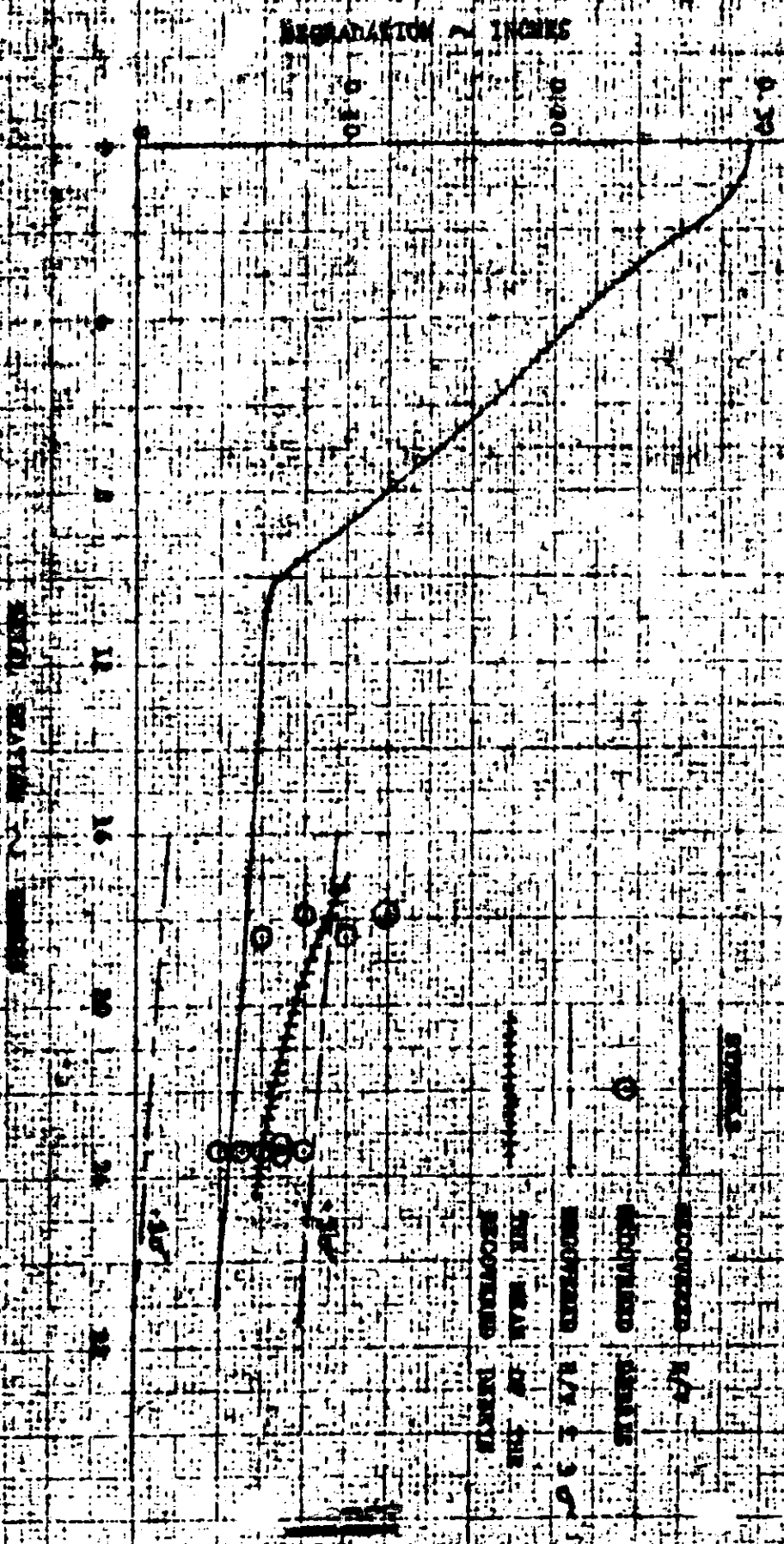
AVERAGE DEPTH
OF DEGRAD.
AT STA. 23.4 = 0.06"

*Axial Distance from stagnation point.

**Based on nominal design thickness: 0.2195"

FIGURE 7

MEASURED SHIELD DEGRADATION VS. AXIAL STAINING



FILE 101 R E B
 SHIELD DEGRADATION IS INTEGRATED HEAT FLUX

DEGRADATION - INCHES

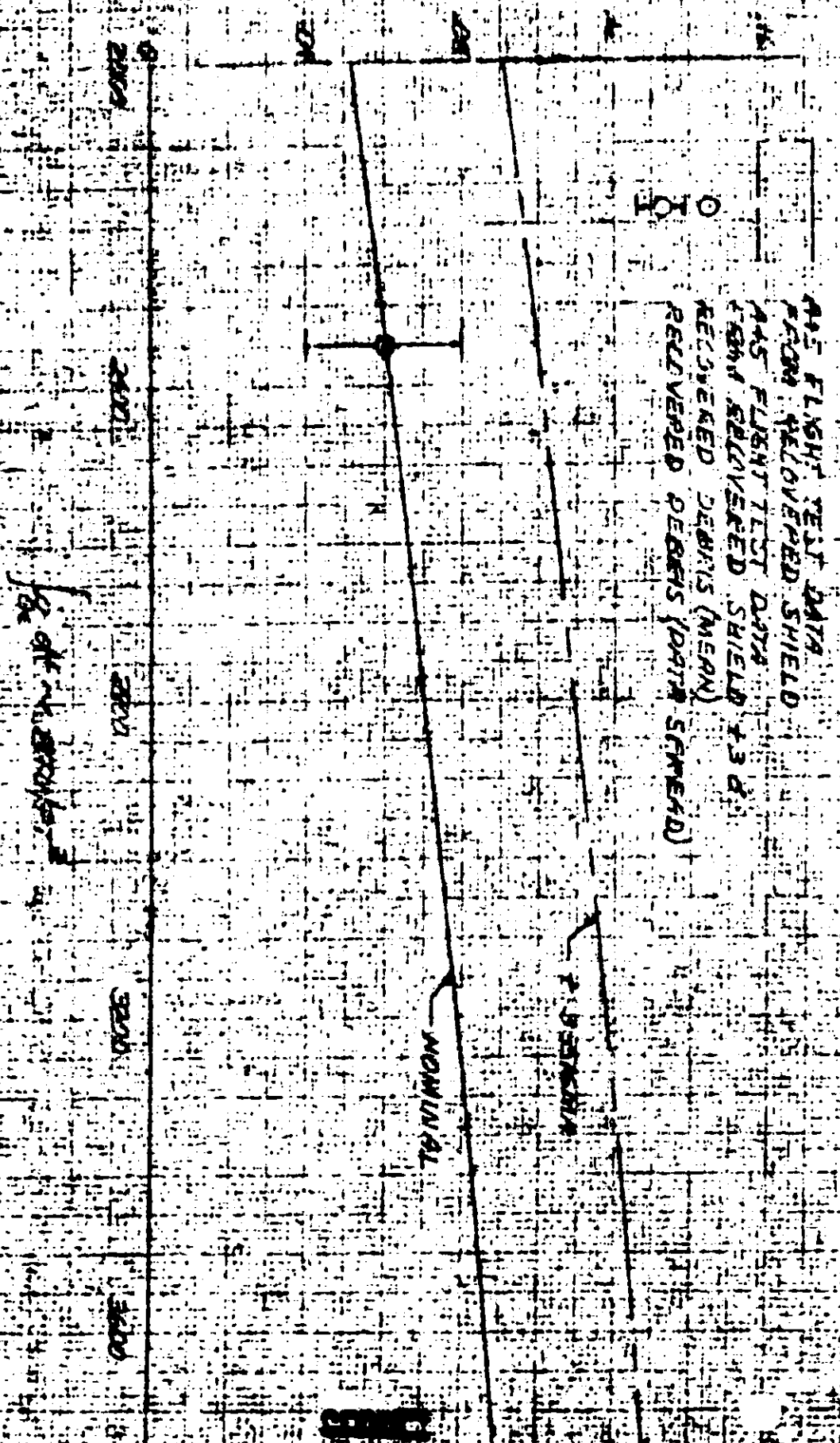


FIGURE 3
 INTEGRATED HEAT FLUX VS ALTITUDE MEANS PARABOLIC

USED
 $U_e = 25,512 \text{ FT/SEC}$
 $T_w = 1600 \text{ }^\circ\text{R}$
 $ALT = 30,000 \text{ FT}$

STATION 18

STATION 20

$\int q dx \sim BTU/FT^2$

2000

2500

3000

REMOVED
 R/V SK

1000 DISTANCE FT

15%

REMARKS

(SIN 0) 45 (COS 0) 45

~~SECRET~~



expected as $q \, dt)_{\text{laminar}} = \frac{1}{2} \rho V^3 \cos^2 \theta$

In order to estimate the possible re-entry path angle extremes indicated by the shield degradation, Figure 9 was developed. This figure presents the dependency of the time integrated re-entry heating as a function of re-entry path angle and ballistic coefficient. Employing the integrated heating obtained from Figure 8 as an argument

$$(\sin \theta)^{-\frac{1}{2}} (W/C_{DA})^{\frac{1}{2}} \quad \text{extremes of 51 and 72}$$

were obtained for Stations 23 and 18 respectively. Assuming a constant hypersonic ballistic coefficient of 55 yields a path angle range of $1^{\circ} 13'$ to $36'$ at an altitude of 325,000 feet. This is a rough estimate of the path angle which fails to take into consideration the vehicle angle of attack and the reported delay of separation of the R/V from the system. Both of these events would cause a significant variation in the vehicle's apparent hypersonic ballistic coefficient.

b. Afterbody Performance

Several portions of the parachute and thermal cover were obtained. The lack of evidence of heating would suggest that these pieces were not exposed to attached boundary layer heating rates. Therefore, it would appear that during the early portion of the re-entry, when normally the R/V has an angle of attack greater than 90° which would cause the occurrence of an attached boundary layer on the thermal cover, the spacer section was still attached to the R/V. Subsequent to the decay of the angle of attack to less than 90° , this member probably was separated from the vehicle, but subsequent chute cover heating rates resulting from wake heating were not high enough to cause significant depolymerization of the Pyroreg cover. This opinion is further substantiated by the condition of the antenna stub and insulated wires exposed in the aft area. None gave an indication of experiencing appreciable heating. An organic film noted on the cover surface is attributed to decomposition products from other materials.

~~SECRET~~

~~SECRET~~

^c
2. Shields

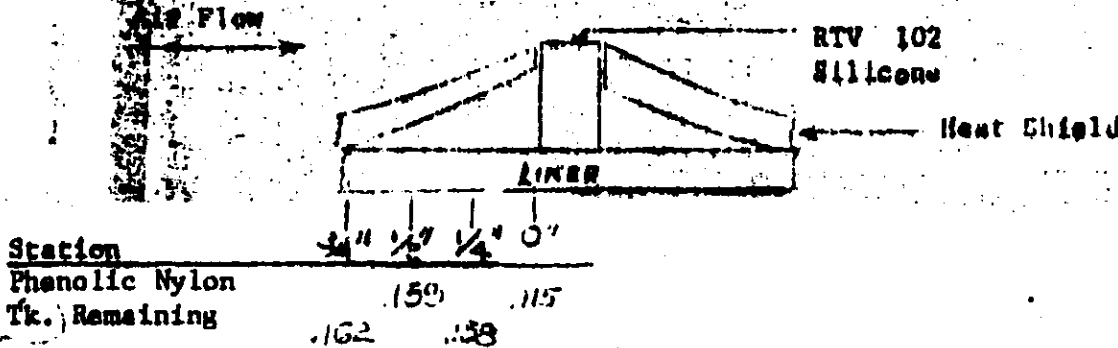
Examination of the aft shield section revealed evidence that cracks were present in the shield during the re-entry heating period. Vertical surfaces of the shield crack were slightly charred down to the phenolic glass liner. These cracks did not alter shield thermodynamic performance.

~~SECRET~~

d. Stress Relief Grooves

A profile view of the saw cut at Station 21 indicated that the local bond between the shield and liner had failed. This resulted in warping or curling of the phenolic nylon shield in the following manner:

FIGURE 10



SKETCH OF SHIELD CROSS-SECTION SHOWING EDGE CURLING

As the remaining thickness of the virgin phenolic nylon decreased ~~as you approached the saw cut~~, it can be concluded that the curvature was present during the heating period. The increased body angle with respect to the air stream resulted in a local pressure and heating increase which lead to greater depths of shield degradation. A similar conclusion was drawn from the recovered R/V 38.

e. Ablative Gap Filler

The ablative gap filler for the recovered debris was RTV 102 silicone ^{rubber}. By comparison of its thermal degradation with that of the phenolic nylon shield it can be concluded that its performance is compatible with the shield material; hence, fully satisfactory for this application. The earlier flights had employed polysulfide ~~PR1221~~ ^{satisfactory} which had also demonstrated thermodynamic performance.

Gap filler adhesion to the phenolic nylon was maintained in the recovered samples. ^{Surface level} Erosion of the RTV 102 was slightly ^{higher} ~~less~~ than that of the phenolic-nylon char remaining on the returned samples. No indications of swelling and void formation as a result of orbital thermal-vacuum or re-entry exposure ^{were} ~~was~~ present.

2. Materials Performance

a. Degradation Kinetics

Thermogravimetric and ^DA_A Differential Thermal Analyses (TGA's and DTA's respectively) were performed to define shield degradation as a function of depth from the surface. Samples were taken from a coring removed from a randomly selected location on the shield skirt. Sample depths were: (1) at the char/virgin material interface, nominally the top third; (2) down 1/16" from (1), nominally the middle third; and (3) down 1/16" from (2), nominally the bottom third. Material from the trim ring of a production heat shield was used as a base reference. Examination of the DTA thermograms Figures ¹¹10 and ¹²11, and ¹³12 show that the top third material does not exhibit an endotherm at $\sim 800^{\circ}\text{F}$, while the deeper samples do in varying degrees. The thermogram of Figure ¹¹10 represents a sampling from the char/virgin material interface. A temperature of 800°F probably corresponds to the "melting" of the phenolic resin, although the exact temperature is a function of curing cycle, etc. The peak at 475°F corresponds to the melting of nylon reinforcement. The intensity of this peak varies with the depth indicating that during re-entry the phenolic resin surface receded approximately 1/16 of an inch.

Thermogravimetric analysis (TGA) curves were run on samples from the same core and depths as the DTA samples. In addition, a reference sample was run to make comparison more complete. The top third curve showed a marked lower residual weight fraction at a given temperature than the ^{deeper or reference samples did.} ~~standard or the unblasted portions of the specimen used:~~ Figures ¹⁴13, ¹⁵14, ¹⁶15, and ¹⁷16 are thermograms of the ^{reference} standard, and top, middle, and bottom thirds of the phenolic-nylon shield samples. Figure ¹⁸17 is a ^{cross-plot} plot of ^{the ratio} (residual weight fraction of the reference material)/(residual fraction of the debris) versus depth, ^{selected} at given temperatures. ^{Data was} taken from the ^{for mentioned} appended TGA curves. Figure ¹⁹18 is a ^{cross-plot of DTA data:} plot of ΔT (the differential temperature of deflection on the ΔT axis) versus depth, ^{selected} at given temperatures for the same material ^{samples}. The same gradation is shown as is in Figure ¹⁹17.

DTA THERMOGRAM OF TOP THIRD PHENOLIC NYLON SAMPLE

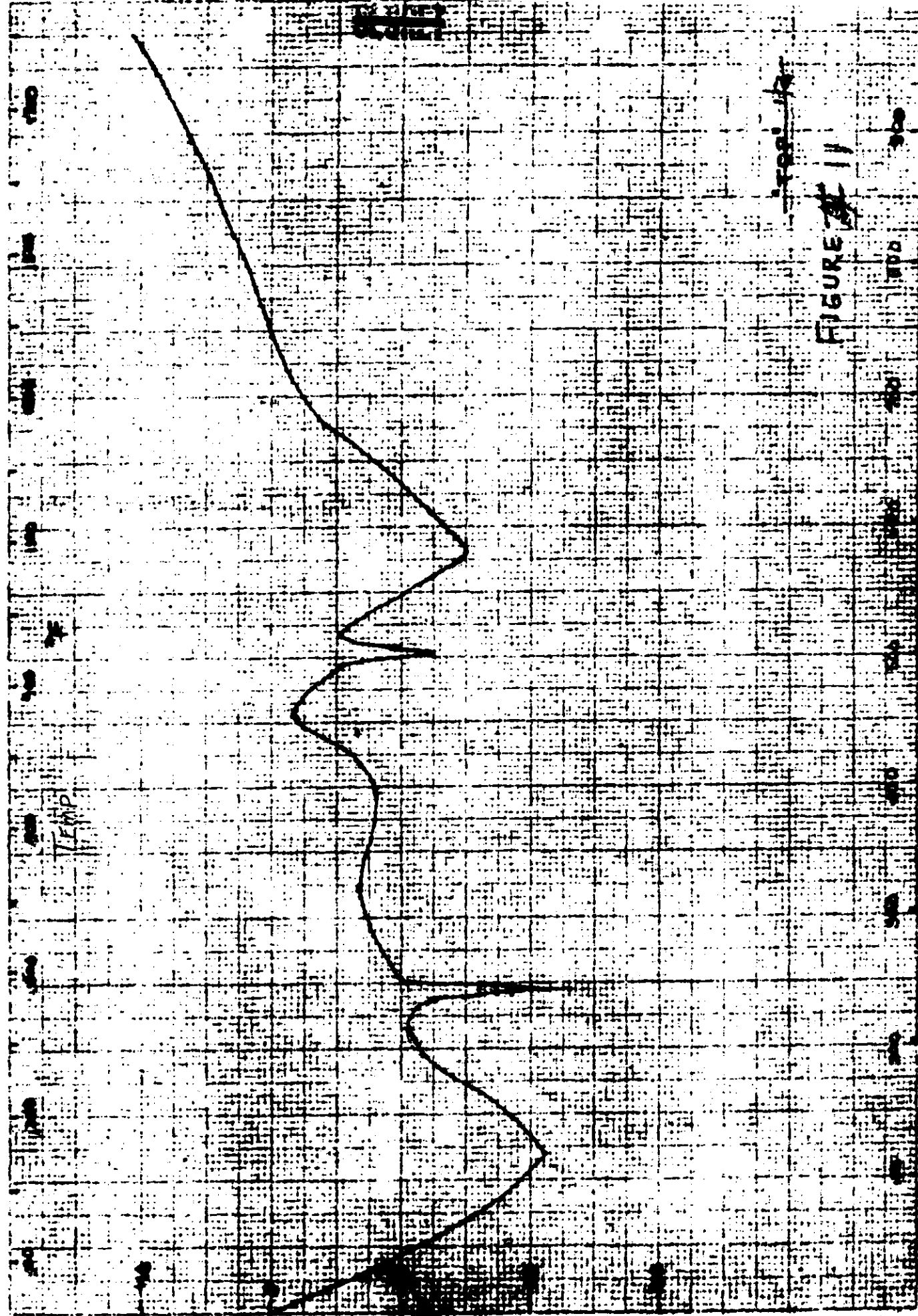
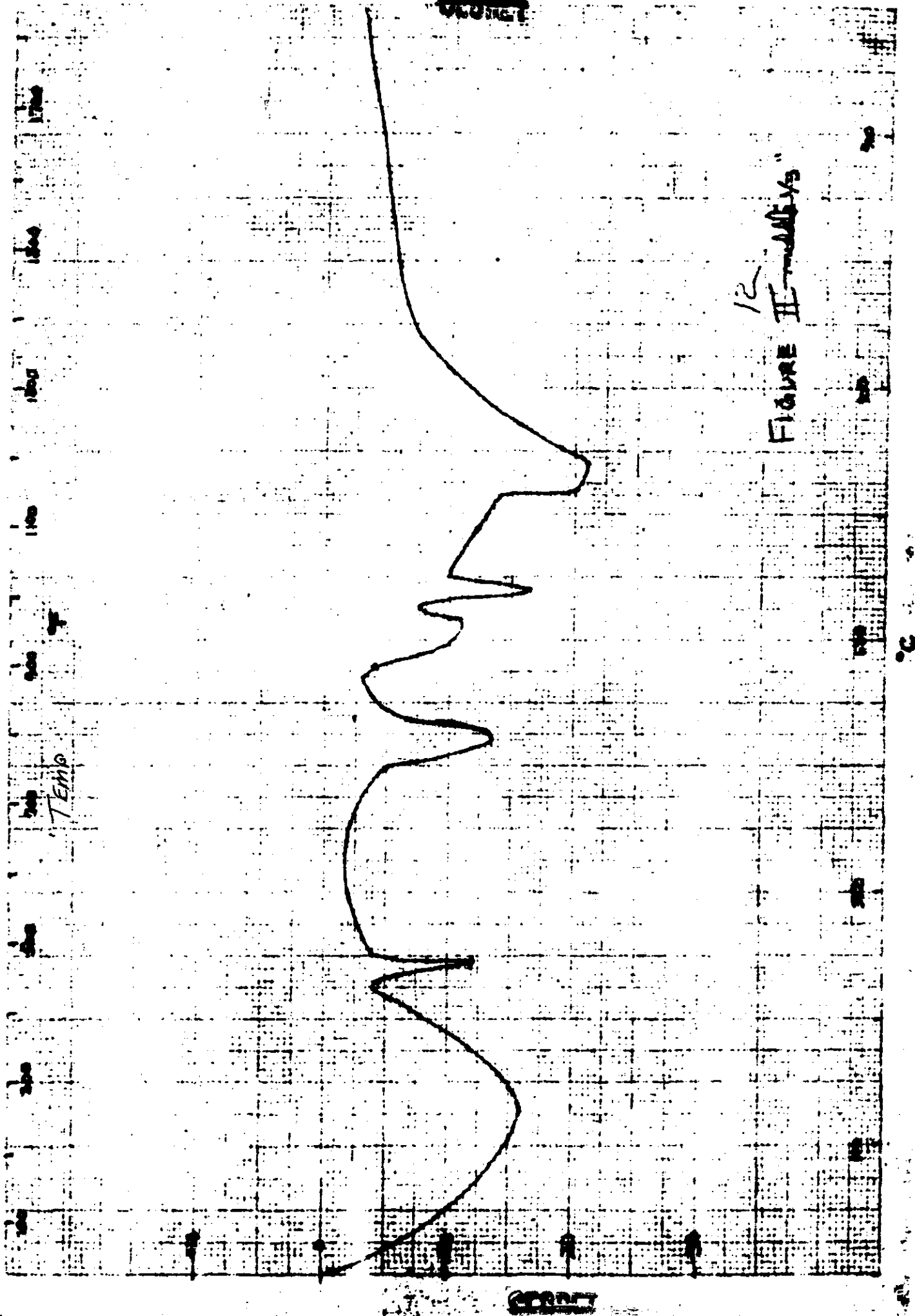


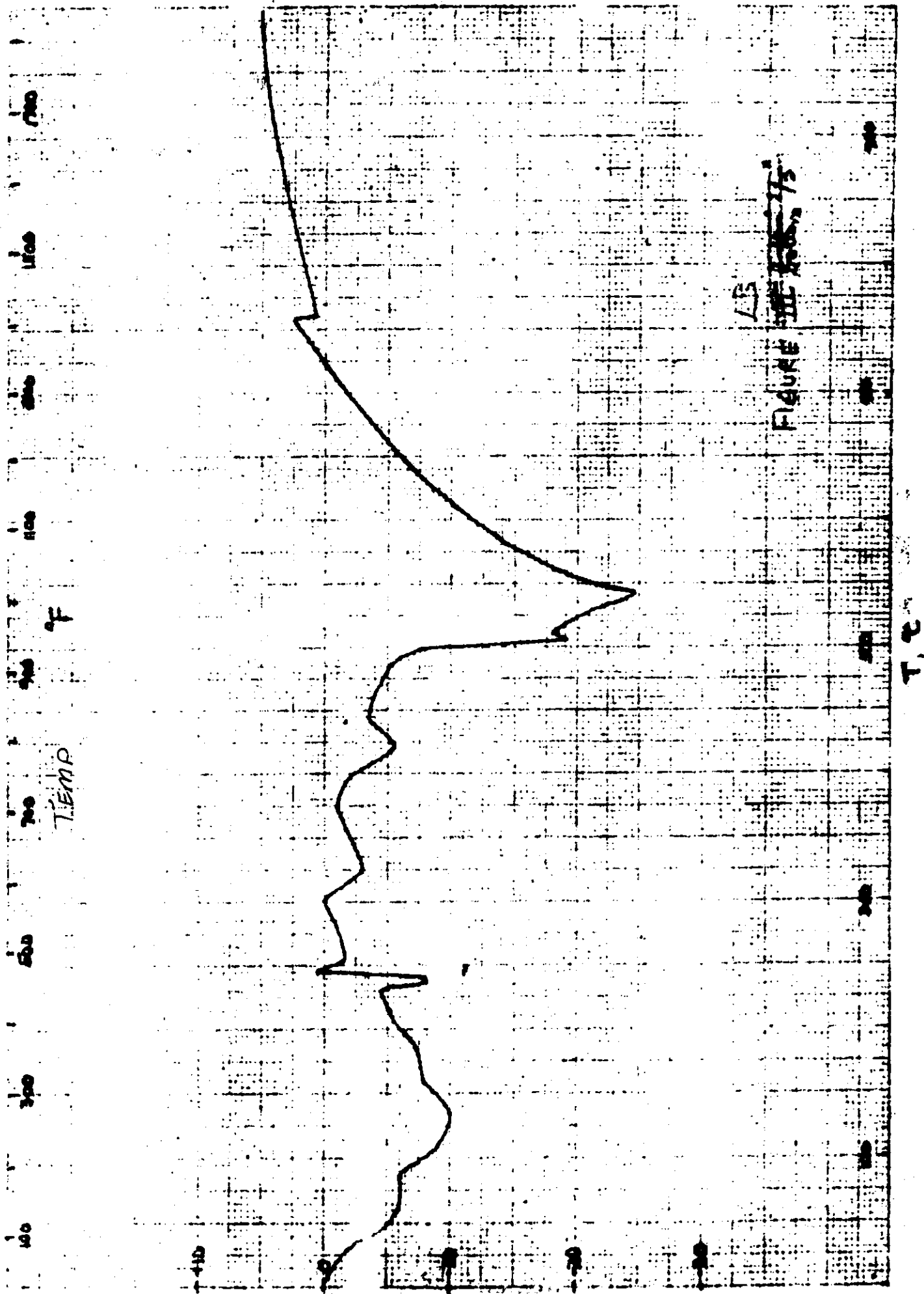
FIGURE 11

DTA THERMOGRAM OF MIDDLE THIRD PHENOLIC - NYLON SAMPLE



12
FIGURE II - ANALYSIS

DTA THERMOGRAM OF BOTTOM THIRD P-N SAMPLE



~~SECRET~~

The local bond separation at the stress relief grooves is probably the result of edge effects early in the environment. However, neither this nor the curling is considered detrimental to the mission performance capability of the system.

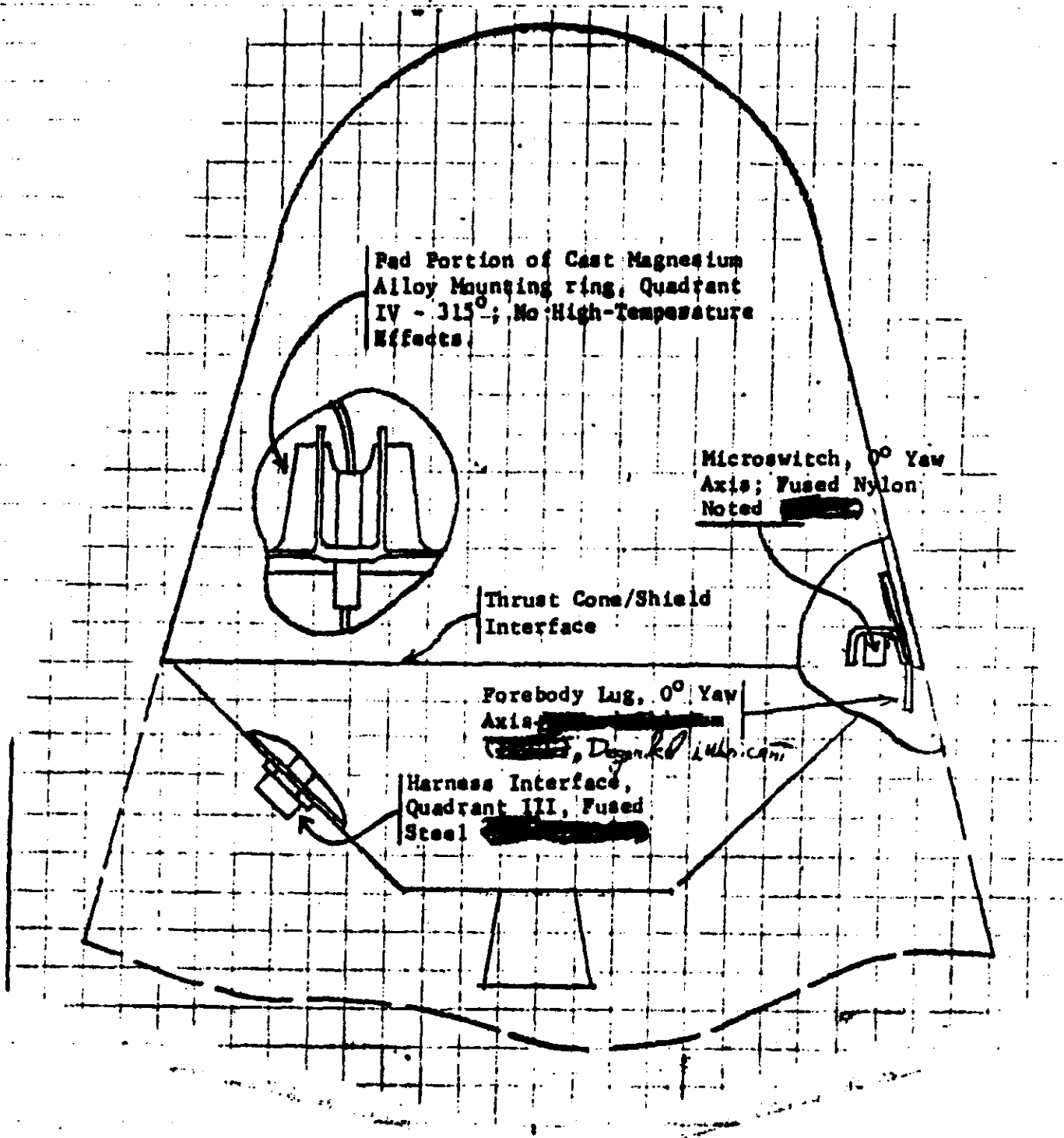
b. Mounting Ring and Capsule Guides

The end tabs of the capsule guides extending between the magnesium mounting ring and the aft shield ring were bent at each location around most of the circumference of the shield (see ^{Figure} ~~Fig.~~ 2 for one of the bent guides). In addition the dowel pin hole elongations extend in the aft direction indicating the magnesium ring moved aft relative to the glass liner. The large guide adjacent to the piston in ^{quadrant} ~~Quad~~-I also had a permanent impression of the raised pad on the magnesium ring, again indicating an aft movement of the ring. The conclusion reached from this is that the shield structure and magnesium ring failed at impact, the capsule structure forcing the magnesium ring aft relative to the glass liner. In addition, the magnesium ring was intact up to the point of impact since, during impact, a uniform circumferential bending of the tabs occurred. This also accounts for the many small pieces of ring since a failure would be expected near each contact point between the magnesium ring and the guides.

Fractures and delaminations noted in the phenolic-glass liner are attributed to impact. Also, no thermal degradation was evident in the M & P 100 ~~epoxy~~-novolac adhesive used for bonding rings and assembly to the phenolic-glass. Cohesive failure was observed in areas of bond separation, indicating that high strength performance was realized in bonded joints.

~~SECRET~~

FIGURE 20



SRV LOCATION OF PARTS. SECTIONED
AND EVALUATED

REPORT

V. CONCLUSIONS

The following conclusions are made based on evaluation of the recovered debris:

1. Cracking of the phenolic-nylon occurred in several places on the heat shield skirt during orbit. These cracks did not alter thermodynamic performance during re-entry. Mission performance adequacy of the shield and structure system was confirmed by flight results.
2. A bulge or protrusion of the phenolic-nylon in the skirt aft ring occurred during orbit ^{or,} more probably, at the start of re-entry heating. A crater-type formation developed during re-entry. Edge "curling" of the phenolic-nylon adjacent to the stress relief grooves was also experienced. Local conditions of these types can be tolerated without effecting mission performance adequacy.
3. Integrity and thermodynamic performance of the new gap filler material was satisfactory.
4. Degradation profile data and degradation rate parameters determined from shield material exposed to the actual re-entry environment will improve confidence and accuracy of degradation and temperature response predictions for future heat shield designs.
5. Heating effects on parts, parachute, and thermal cover materials evaluated indicate that afterbody heating was small. This suggests that the afterbody was not directly exposed to the aerothermodynamic heating environment during re-entry while tumbling, or prior to R/V stabilization and separation. Apparently the adapter protected the R/V afterbody during the initial period of re-entry heating.
6. The magnesium mounting ring and ring-to-liner bond did not experience excessive temperatures during re-entry. Mounting ring and bond maintained integrity until impact. Cohesive bond failures and predictable ring failures occurred on impact.

7. Shield degradation during re-entry matched semi-empirical correlations based on previous flight data within reasonable assumption of tolerances.
8. Adequacy of the present vehicle design and quality was confirmed.

~~SECRET~~

VI. REFERENCES

1. PIR SM-8156-475, "Final Thermal Stress Analysis of H30 Re-entry Vehicle" by [REDACTED] 9/24/63 (S)
2. TIS R58SD227, "Thermodynamic Analysis", by [REDACTED] January, 1958.
A Summary of the Aerodynamic and Thermodynamic Data for the H30 Re-entry Vehicle
Report of the H30 Re-entry Vehicle Team
Approved for Release
3. [REDACTED] Journal of Polymer Science, Part A, 2, 3147-3151 (1964)

~~SECRET~~

3. Structural Performance

a. Heat Shield

The center portion of Figure 1 shows an area where the phenolic-nylon is completely ablated away in a local crater shape. ~~The phenolic-nylon is completely ablated away in a local crater shape.~~ The phenolic-nylon is separated from the phenolic glass liner underneath the crater type formation. This type of formation is probably the result of a local unbonded region between the phenolic nylon and the phenolic glass liner. Either due to elevated temperatures in orbit or during a shallow re-entry, the hoop and axial compressive thermal loading in the phenolic nylon can cause such protuberances which ablate ^{rapidly} more than the surrounding area, until ablating through in the center. Pressure from entrapped volatiles might also be a factor in the formation. Subsequent ablation would develop the crater type erosion. The present unbonded area is estimated to be about 2 inches in diameter. Local unbonded areas of this size, however, can be tolerated without affecting the mission performance capability of the structural system.

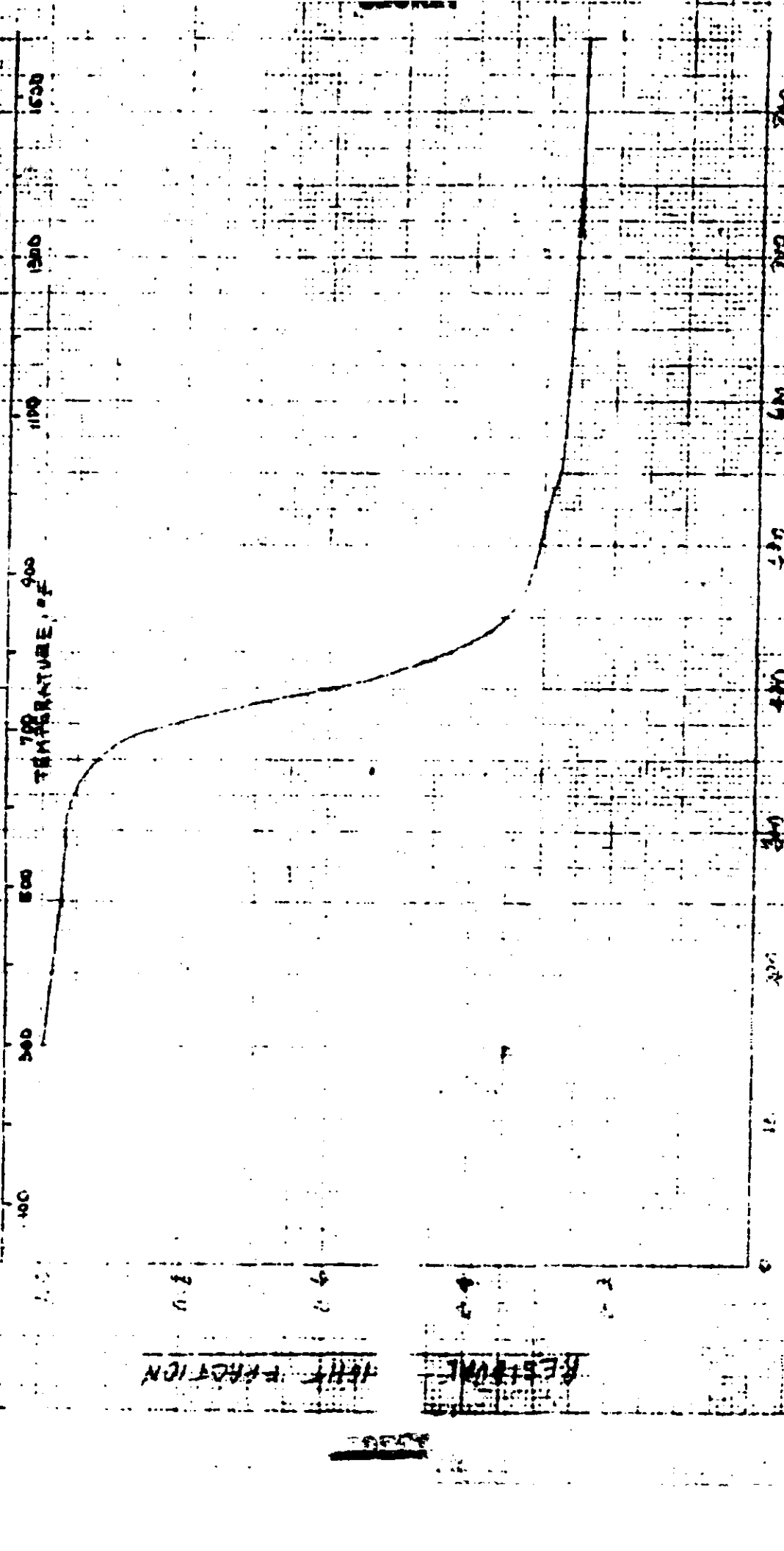
In Figure 2, a local bond separation at the edge of the ^{stress relief groove} ~~saw-out~~ is evident, with the phenolic nylon curled ^I upon the free edges. The virgin nylon thickness tapers off as the ^{stress relief groove} ~~saw-out~~ edge is approached.

The curling phenomena can occur from high temperature exposure during orbit or re-entry. It is caused by the difference in thermal expansion between the unrestrained phenolic-nylon (unbonded) and the adjacent phenolic-nylon restrained by the bond to the liner. However, sufficient time and temperature are required to permit inelastic creep deformation to occur.

During the orbit environment, where the local high temperature reaches 250°F, many orbits would be required to produce this effect, as the temperature is relatively low. During reentry, when the phenolic-nylon reaches temperatures around 700°F, a much shorter time will produce the same effect. Of the two environments, reentry is considered to be the most probable source due to the circumferential symmetry of the curl. Once the curling phenomena has occurred, subsequent ablation will even off the local ^{flare} protrusion giving the tapered shape seen in Figure 2.

1011 - THE KIMBERLY OF DALLAS (MID 19th century)

~~Actual Name: 3.1. DONT~~



TEMPERATURE °C

100

IGA THERMOGRAM OF TOP THIN PN SAMPLE

AFRICAN MODEL, TOP THIN

0.0

0.8

TOP TEMPERATURE °F

500

1000

1500

2000

2500

3000

3500

4000

4500

5000

5500

6000

6500

7000

7500

8000

8500

9000

9500

10000

10500

11000

11500

12000

12500

13000

13500

14000

14500

15000

15500

16000

16500

17000

17500

18000

18500

19000

19500

20000

20500

21000

21500

22000

22500

23000

23500

24000

24500

25000

25500

26000

26500

27000

27500

28000

28500

29000

29500

30000

30500

31000

31500

32000

32500

33000

33500

34000

34500

35000

35500

36000

36500

37000

37500

38000

38500

39000

39500

40000

40500

41000

41500

42000

42500

43000

43500

44000

44500

45000

45500

46000

46500

47000

47500

48000

48500

49000

49500

50000

50500

51000

51500

52000

52500

53000

53500

54000

54500

55000

55500

56000

56500

57000

57500

58000

58500

59000

59500

60000

60500

61000

61500

62000

62500

63000

63500

64000

64500

65000

65500

66000

66500

67000

67500

68000

68500

69000

69500

70000

70500

71000

71500

72000

72500

73000

73500

74000

74500

75000

75500

76000

76500

77000

77500

78000

78500

79000

79500

80000

80500

81000

81500

82000

82500

83000

83500

84000

84500

85000

85500

86000

86500

87000

87500

88000

88500

89000

89500

90000

90500

91000

91500

92000

92500

93000

93500

94000

94500

95000

95500

96000

96500

97000

97500

98000

98500

99000

99500

100000

100500

101000

101500

102000

102500

103000

103500

104000

104500

105000

105500

106000

106500

107000

107500

108000

108500

109000

109500

110000

110500

111000

111500

112000

112500

113000

113500

114000

114500

115000

115500

116000

116500

117000

117500

118000

118500

119000

119500

120000

120500

121000

121500

122000

122500

123000

123500

124000

124500

125000

125500

126000

126500

127000

127500

128000

128500

129000

129500

130000

130500

131000

131500

132000

132500

133000

133500

134000

134500

135000

135500

136000

136500

137000

137500

138000

138500

139000

139500

140000

140500

141000

141500

142000

142500

143000

143500

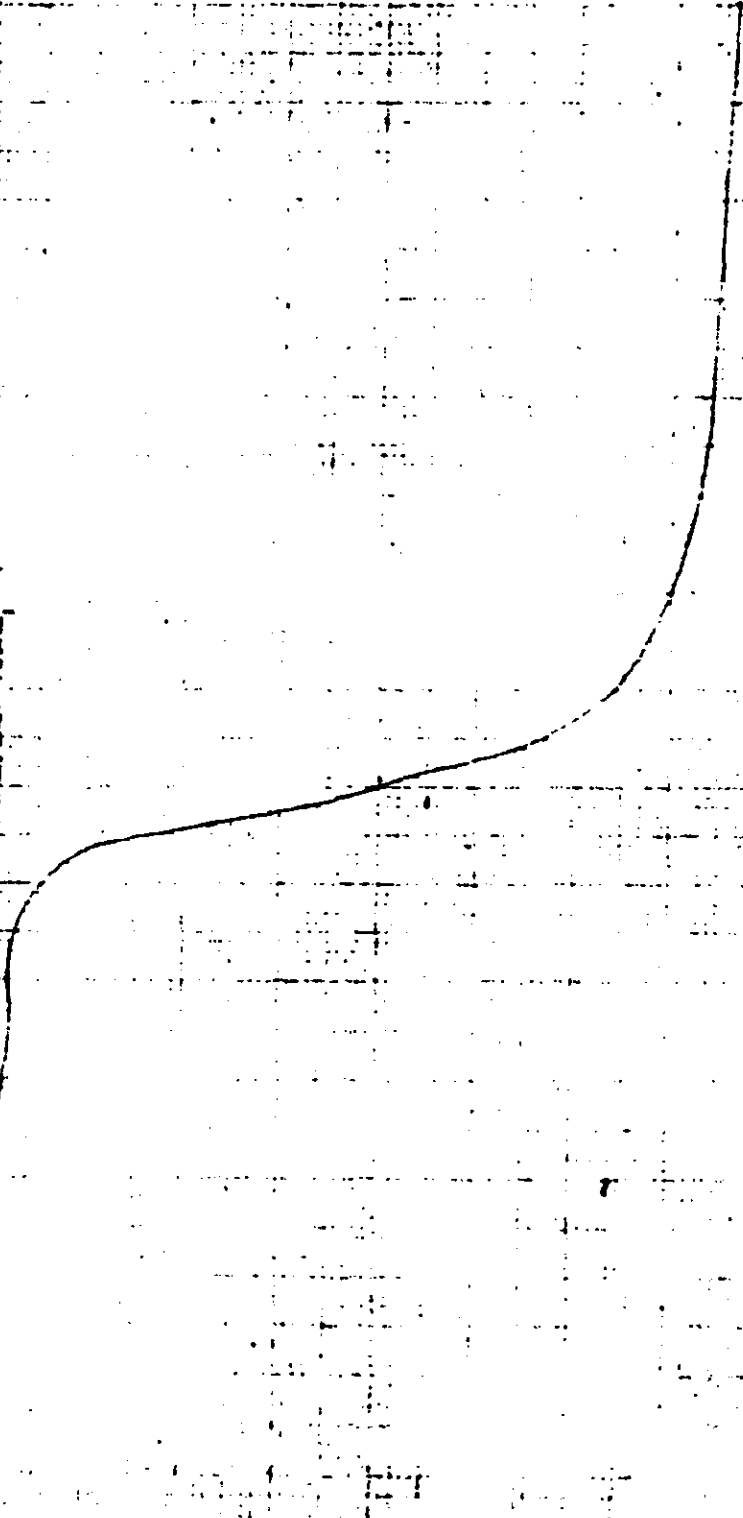
144000

1. GH THERMOGRAM OF MIDDLE HIRD PN SAMPLE

AFRICAN AIR FORCE 73 1024N

100 200 300 400 500 600 700 800 900 1000 1100 1200 1300 1400 1500

PERCENTAGE OF



100 200 300 400 500 600 700 800 900 1000 1100 1200 1300 1400 1500

TEMPERATURE IN °C

FIGURE 15

TGA THERMOGRAM OF REF. A SAMPLE

STANDARD FOR D-065

TEMPERATURE, °F

TEMPERATURE, °C

WEIGHT, %

TIME, MIN

DATE

TIME



DATE

TIME



DATE

TIME



DATE

TIME



DATE

TIME



DATE

TIME



DATE

TIME



DATE

TIME



DATE

TIME



DATE

TIME



DATE

TIME



DATE

TIME



DATE

TIME



DATE

TIME



DATE

TIME



DATE

TIME



DATE

TIME



DATE

TIME



DATE

TIME



DATE

TIME



DATE

TIME



DATE

TIME



DATE

TIME



DATE

TIME



DATE

TIME



DATE

TIME



DATE

TIME



DATE

TIME



DATE

TIME



DATE

TIME



DATE

TIME



DATE

TIME



DATE

TIME



DATE

TIME



DATE

TIME



DATE

TIME



DATE

TIME



DATE

TIME



SECRET

RESIDUAL WT. FRACTION STANDARD / RESIDUAL WT. FRACTION SLAB

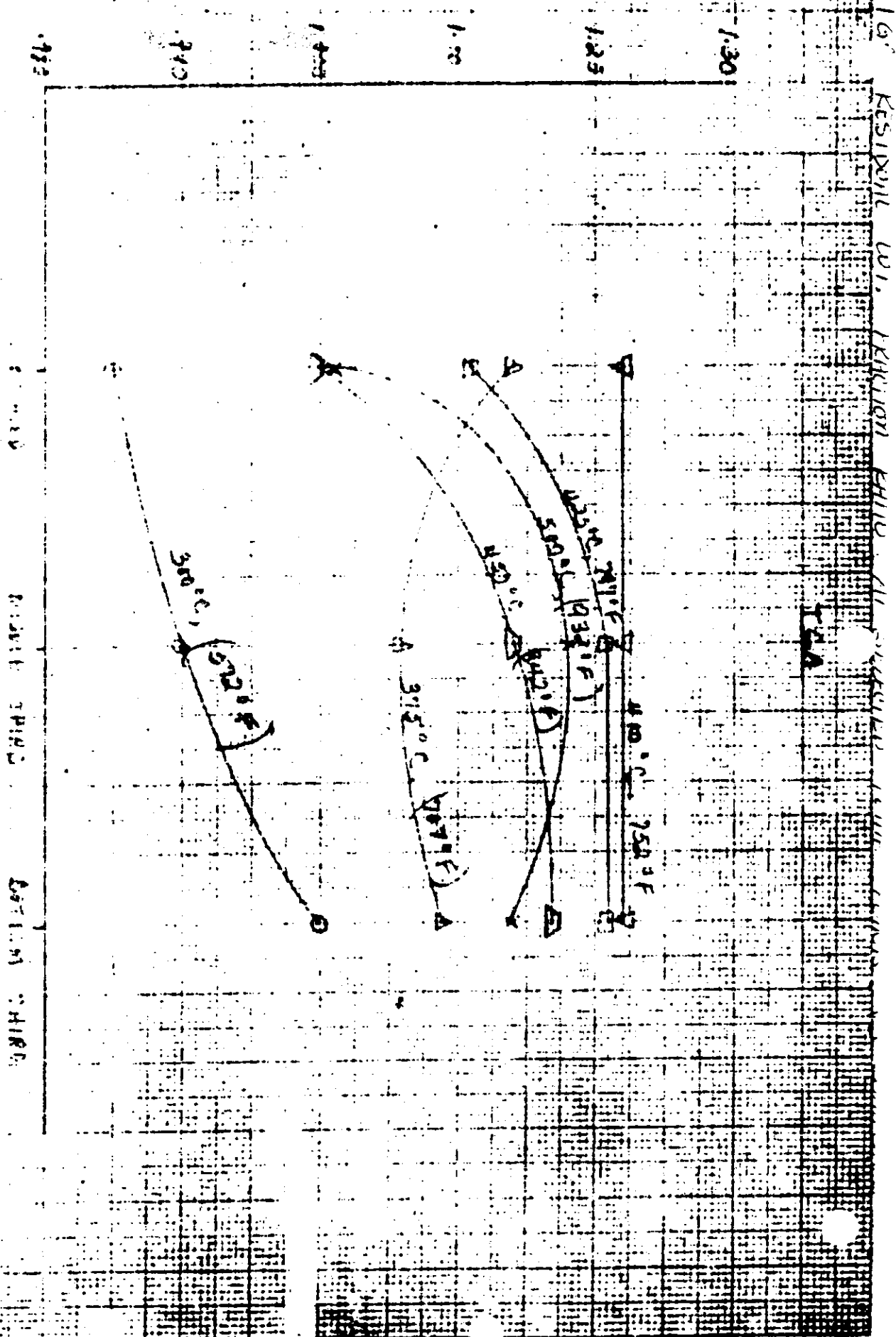
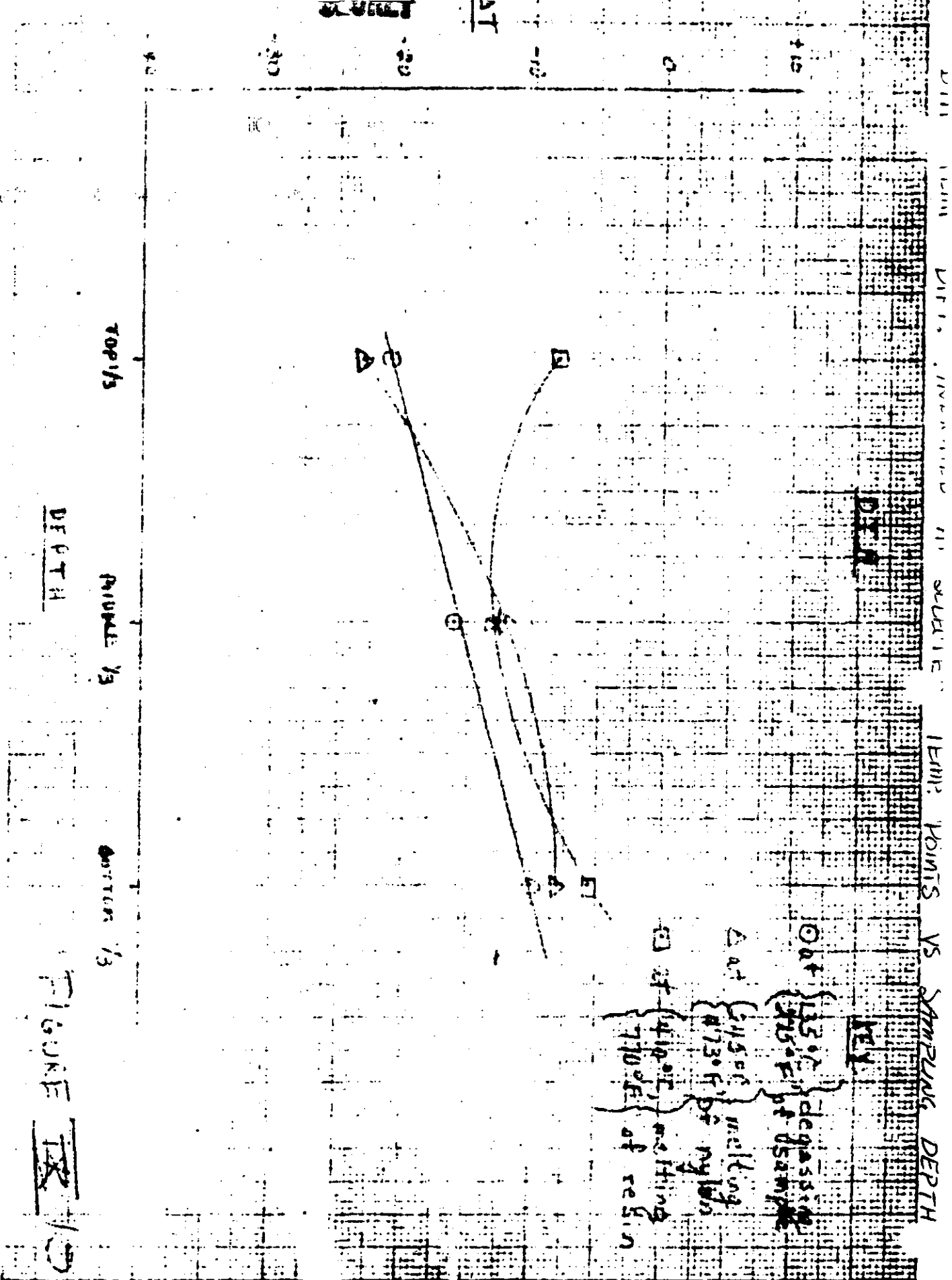


FIGURE 15

SECRET



DEPTH

FIGURE 18

Making the reasonable assumption that the reference sample used in this work is ^{representative of the}
 recovered phenolic-nylon ^{before flight} ~~manufactured~~ (representative as used here means
 that both parts experienced approximately the same cure), then ^{The data shows that the} ~~one can say the~~
 most severe gradation of properties occurs from the surface (top third) to 1/16
 inch below it (middle third). That is, ~~DTA and TGA~~ DTA and TGA showed the greatest
 change of property in that region as opposed ^{change from} ~~to the middle third to bottom~~ ^{the}
 or bottom ^{third} to reference samples. Reference to Figure ^{is particularly} 17 shows this to be true,
 especially in the region from 797°F to 932°F.

The Arrhenius equation

$$K = Ae^{-E_a/RT}$$

provides the rational model currently used for predicting material response to
 high heating rate (re-entry) environments.

Arrhenius parameters were calculated from the TGA data using the method of Fuoss,
 Salyer, and Wilson. Results for the three different layers are presented in

Table II below:

TABLE II

ARRHENIUS PARAMETERS

	Reaction Order (n)	- E _{act} (in kcal/mole)	Collision Frequency (A) (in sec ⁻¹)
Top Third of Debris	1	15.7	1.39 x 10 ²
	2	31.4	6.45 x 10 ⁵
Middle Third of Debris	1	17.8	6.6 x 10 ²
	2	35.6	1.34 x 10 ⁷
Bottom Third of Debris	1	18.8	1.26 x 10 ³

Reference Phenolic
Nylon

1
2

21.3
42.6

6.78×10^3
 1.409×10^9

An examination of the table indicates that the parameters differ for the three ~~levels of debris~~ ^{samples and the reference} sample. Beginning at the top layer and proceeding through ^{reference} the material, a gradual increase in both activation energy and collision frequency may be noted, but the increase is slight. Increase in both parameters is monotonic from top to bottom to reference (unexposed) material.

b. Parts Evaluations

Four parts from the recovered vehicle debris were sectioned and examined for indications of deterioration due to orbit, re-entry, and/or ambient exposure. The four parts were a microswitch (692D911), forebody ^{lug} (10287805), ^{int. face} ~~harness~~ ^{harness} connector (W1J1), and a portion of the cast magnesium alloy ~~(100R306)~~ ^(198R301) mounting ring. All evidence indicated that the parts had performed satisfactorily. Fused materials were identified and the minimum operating temperatures were estimated.

Figure ²⁰ 15 is a schematic showing the location of the parts. The three items on the aft end of the vehicle showed indications of high temperature deterioration, whereas the cast magnesium alloy mounting ring, which is located approximately eight inches forward of the shield/thrust cone interface showed no signs of high temperature deterioration. Indications of corrosion apparently due to weathering, and not considered excessive for ^{Tropical} ~~the 30-day~~ exposure, were noted on the harness interface, forebody lug, and magnesium ring.

1. Microswitch (692D911)

The microswitch with an aluminum alloy angle bracket was removed from the R/V for examination; 5½ inches of the lead wires (three in all) was also retained including a nylon fastener. The microswitch was located at the thrust cone/shield interface; two switches were used in the vehicle assembly and were located 180° apart in proximity to the yaw axis. The switch under consideration was at 0° yaw axis.

The aluminum alloy angle bracket with its two bolts showed no signs of melting or deterioration. The casing of the microswitch had survived the environment and was discolored with a superficial coating of decomposition products emanating from adjacent materials. The plunger of the switch showed the same superficial coating; the seal between the plunger and the silicone rubber bellows and between the bellows and the casing had deteriorated. The bolts attaching the switch to the angle were in good condition.

The potting material had cracked such that the terminals for three lead wires were exposed. No melting of the solder was noted.

The lead wires showed no deterioration of the outer braid. A nylon attachment loop had fused onto the wires and onto a bolt. Lacing cord on the wires also had indications of incipient melting.

The evidence of the fused nylon indicates an exposure to a temperature of approximately 475°F. ~~The~~ Lack of melting of the soldered terminals further indicates short-time exposure. The solder melts at 350°F and the casing and potting material would protect the terminals during a short time thermal exposure.

2. Forebody Lug (102B7805)

The forebody lug, measuring $4\frac{1}{2}$ x $\frac{1}{2}$ x $\frac{1}{8}$ inches which was attached to the aft end on the edge of the vehicle with a 2 inch projection outside the thrust cone assembly. The lug was located at 0° yaw axis.

Evidence of thermal exposure of this first 2 inch section was noted as severe degradation of the dry film lubricant alkyl binder, and had the beaded appearance of weld spatter. The next $1\frac{3}{8}$ inches of the lug showed a gradual change to a less degraded condition. Adherence of the coating exhibited progressively less deterioration along this section of the lug. The remainder of the lug was unaffected. The only portion where corrosion was noted was the middle section. The quantity of rust was small.

SECRET

3. WJ1 Interface Harness Connector [REDACTED] PC07H-22-55P)

The harness interface showed fusion of the steel shell along one edge with some flaring. The remaining connector pins of the harness were held in place by the fused glass-bonded mica insert. The harness shell was also rusted indicating that a protective cadmium plating had been vaporized.

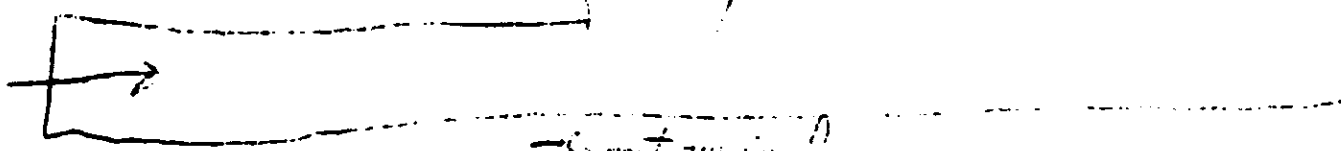
The indications are that this part was heated to a ~~minimum~~ temperature of approximately ~~range~~ 3000°F, causing the observed fusion of metal. The time of exposure can be estimated as short (~5 minutes).

4. Mounting Ring (198R306)

A representative sample of the magnesium ring (ZE41A alloy) was taken as two sections; the pad portion with the explosive bolt/piston assembly, and an adjacent portion of the ring. The sectioned part was located in quadrant IV.

The ring portion contained a steel dowel pin and an attached piece of ~~metallic~~ lead measuring 1 5/8 x 3/4 x 1/2 inches. The lead slug was attached with a cadmium plated steel bolt which showed some discoloration. The dowel pin was rusted and deep pitting was noted in the adjacent magnesium material indicating a galvanic corrosion mechanism in this area. *The exposed... next to A line*

an
A



The pad is a complex shape, and had attachments of the explosive bolt/piston assembly, five epoxy/fiber studs, and a slug of lead attached with a cadmium plated steel bolt. The lead slug was 2 x 3/4 x 1/2 inches and was bent into a shallow "vee" shape with the bolt at the apex. The lead showed no deterioration. The five epoxy/fiber studs at the shield/structure interface were in excellent condition. This entire surface was in good condition indicating that the adhesive (M&P 100) afforded sufficient protection.

Cut A

Insert Where Indicated

The ^{exposed interior surface} magnesium ring was painted with black enamel. Underneath the paint, the ring had corroded producing a heavy white oxide which had lifted the paint in several places

VII. SYMBOLS

A = collision frequency

E_{act} = activation energy

n = order of reaction

R = constant

W = instantaneous weight

W_0 = initial weight

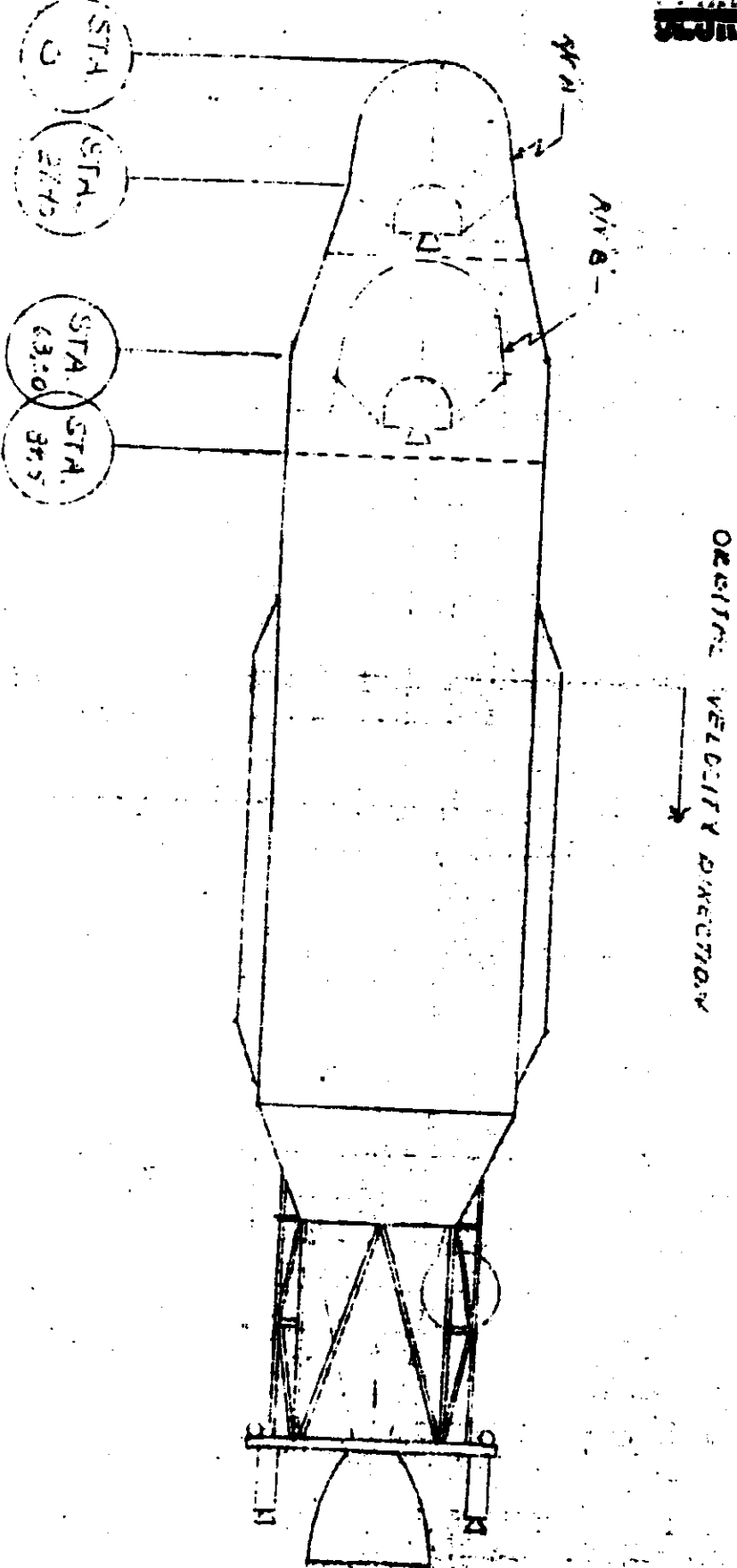
W_f = final weight

T = absolute temperature

The exterior portion of the explosive bolt/piston assembly is fabricated from an aluminum alloy and had survived the environment. The piston section was discolored with a loose black scale. That portion of the pad that the explosive bolt was attached to ^{showed} ~~show~~ extensive corrosion and particles of ~~ea~~ ^{impacted} indicating that the part was buried in the ground or had ~~impact~~ ^{impacted} on that area. A portion of the pad that was at the shield ^Istructure interface had fracture on impact. Four anodized aluminum rivets were located in the web portion of the pad and no deterioration of these rivets was noted.

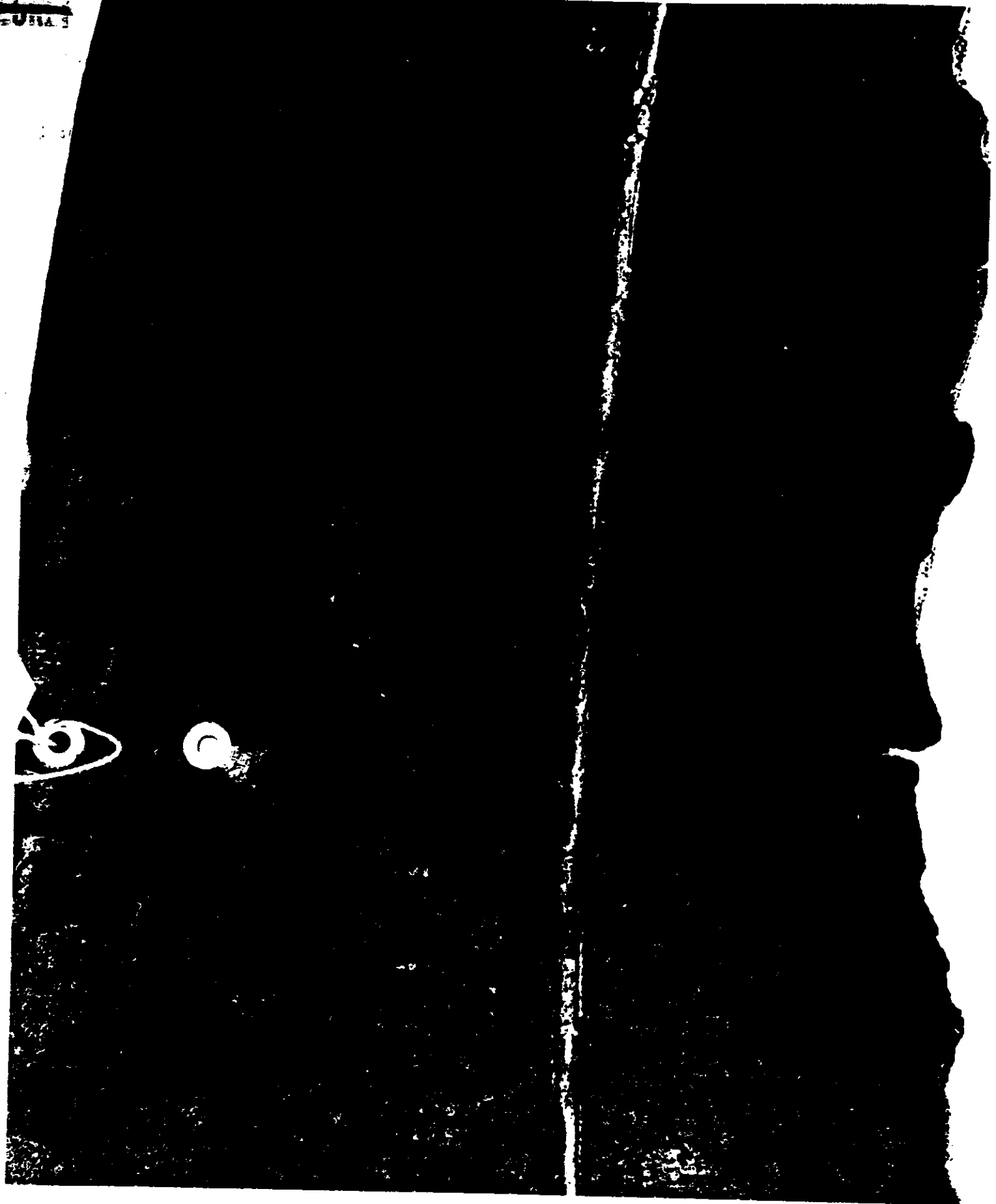
No indications of fusion were noted on the magnesium alloy mounting ring or its attachments. Corrosion of the magnesium was not considered excessive for type of environmental exposure and physical condition of the ring. Maximum temperatures of the magnesium ring section were not excessive. ~~XXXXXXXXXX~~

SECRET



SECRET

UHA 1

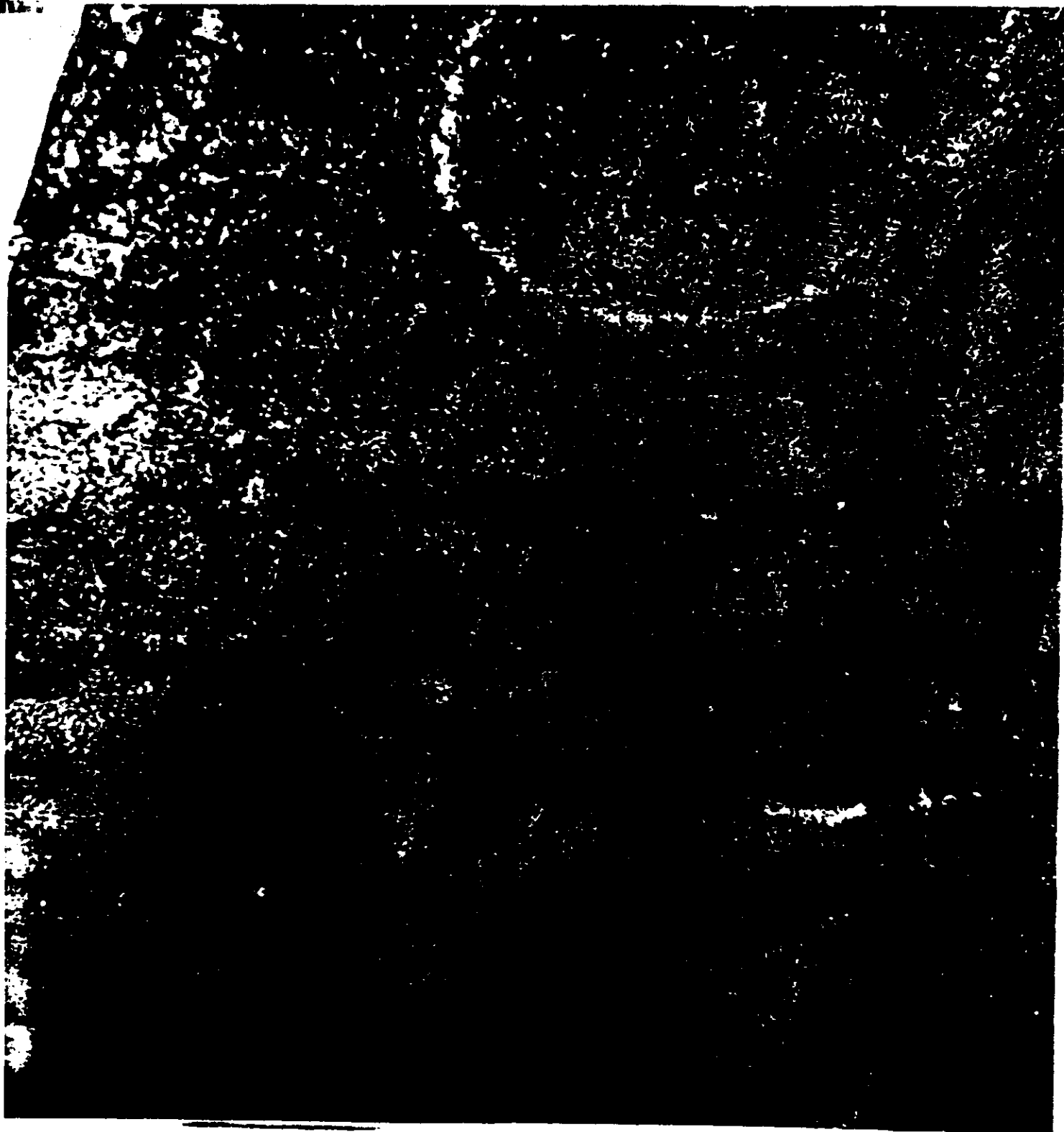


00000

SECRET



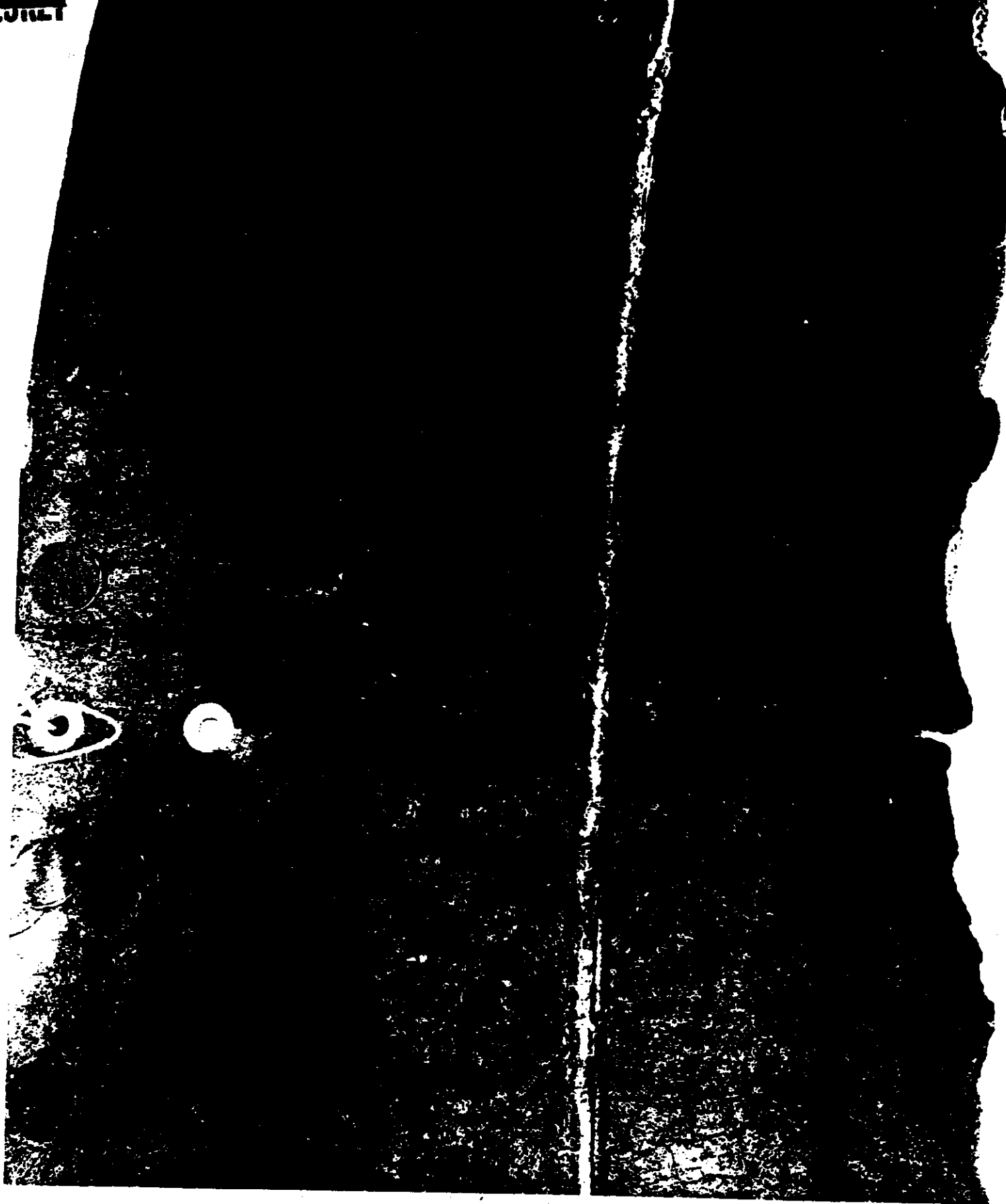
SECRET



2

3

SECRET



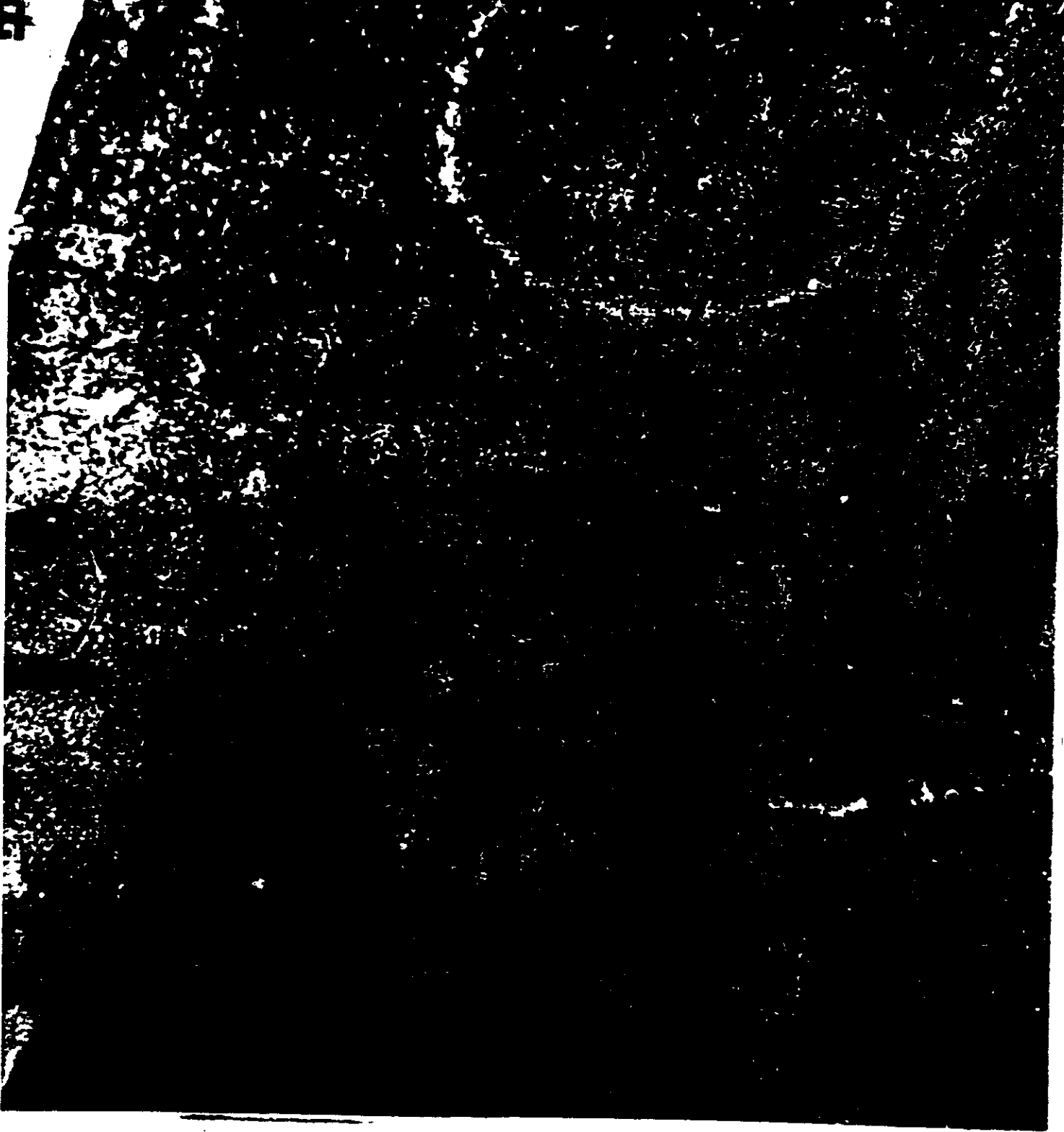
SECRET

SECRET



SECRET

~~SECRET~~

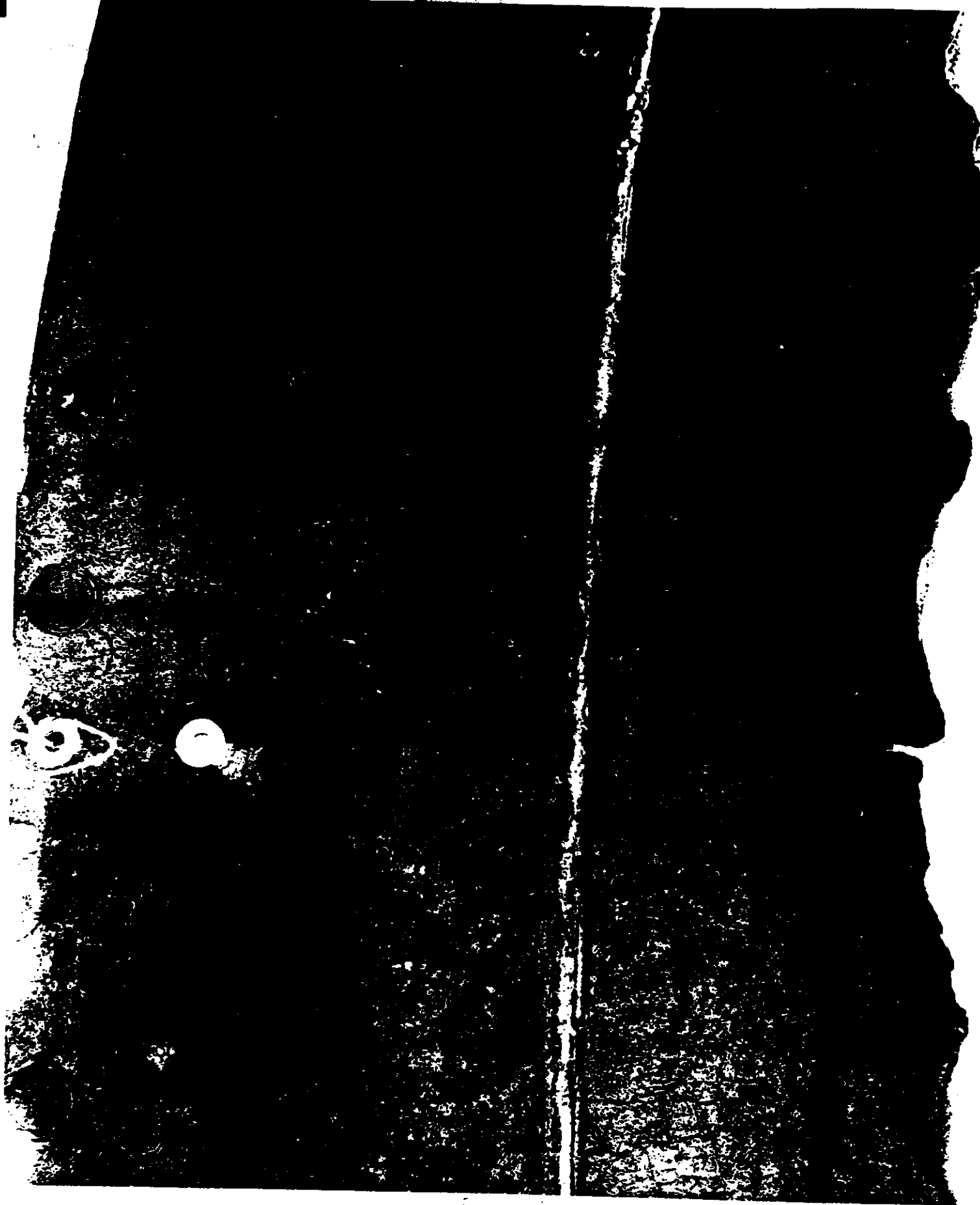


2

3

File

~~SECRET~~



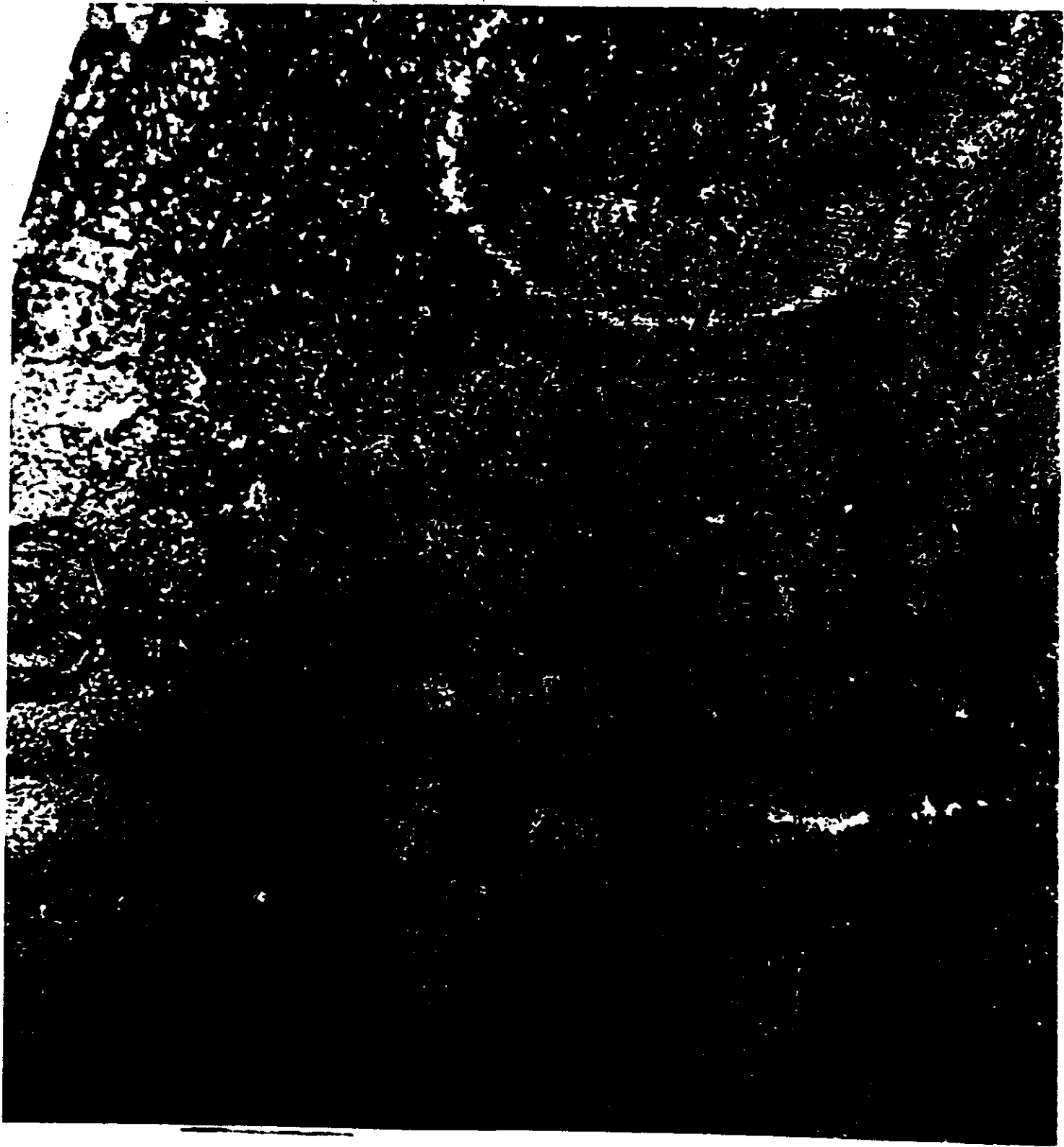
SECRET



F. 1. 2

1100

SECRET



2

3

SECRET

